Nd MODEL AGE MAPPING IN THE GRENVILLE PROVINCE (MATTAWA REGION)

THE EVOLUTION OF THE GRENVILLE PROVINCE IN THE MATTAWA REGION OF ONTARIO: EVIDENCE FROM NEODYMIUM AND CONSTRAINTS FROM AEROMAGNETIC DATA

By

MICHAEL K. HERRELL, B.Sc. (Hons.)

A Thesis

Submitted to the School of Graduate Studies

In Partial Fulfillment of the Requirements

for the Degree

Master of Science

McMaster University

April 2002

Master of Science (Geology)

McMaster University Hamilton, Ontario

Title: The Evolution of the Grenville Province in the Mattawa Region of Ontario: Evidence from Neodymium and Constraints from Aeromagnetic Data.

Author: Michael K. Herrell
Honours B.Sc. (McMaster University)

Supervisor: Professor Alan P. Dickin

Number of Pages: xi, 94

ABSTRACT

Approximately eighty new neodymium model ages were determined on grey orthogneisses in the Mattawa region of Ontario and were used to develop a Grenvillian tectonic model in the region. A residual-magnetic field map developed from aeromagnetic data provides an additional constraint on the terranes mapped based on Nd-model ages. The field area was divided into three sections: the northern section, the Mattawa klippe, and the southern section.

The objectives of mapping in the northern section were two-fold: 1) to map the location of erosional remnants of the allochthon boundary thrust (ABT) and 2) to test the hypothesis that northwestward thrusting of the ABT over the parautochthonous belt caused décollement of a magmatically reworked Archean terrane, creating a duplex thrust sheet and consequent northwestward thrusting of the magmatically reworked Archean parautochthon.

Two allochthonous units previously mapped in this region are the Lac Watson nappe and the Lac Booth klippe. These allochthonous units, characterized by Nd-model ages <1.8 Ga are bound by a magmatically reworked Archean terrane (referred to as the reworked Archean parautochthon) with a Nd-model age range of 1.9-2.6 Ga. Likewise, the perimeter of the reworked Archean parautochthon is truncated by a pristine Archean

terrane which exclusively hosts Nd-model ages > 2.6 Ga, indicating that there are three crustal stacking levels in the northern section.

Nd-model age mapping was employed in the Mattawa klippe region with the same objectives as in the northern section and additionally to provide constraints on the methodology that is to be used when mapping first-order tectonic boundaries such as the ABT. Ketchum and Davidson (2000) suggested that the ABT trended northward in this region based on the presence of 1.16 Ga coronitic metagabbros which Ketchum (1994) concluded were exclusively confined to the allochthonous polycyclic belt (APB). It was determined here that although the metagabbros are confined to allochthonous crust, based on Nd-model ages, they are contained within an allochthonous klippe (Mattawa klippe) overlying the reworked Archean parautochthon, that transported the coronitic metagabbros northwestward. Therefore, this klippe represents an erosional remnant of the APB but the main ABT is located further south.

Nd-model age mapping in the southern region identified three distinct crustal terranes. The Mattawa fault was determined to be a brittle fault following approximately along a pre-Grenvillian suture. This separates the reworked Archean parautochthon from the Paleoproterozoic parautochthon, which had a Nd-model age range from 1.8-1.9 Ga. The Paleoproterozoic parautochthon was found to be truncated by the main body of the APB, containing Nd-model ages < 1.8 Ga. The boundary between the Paleoproterozoic parautochthon and the APB was interpreted as the location of the main ABT.

Based on the distribution of Nd-model ages in the region, four distinct crustal terranes were identified representing two thrusting events. Initially the ABT was overthrust on the parautochthonous belt causing décollement of the reworked Archean parautochthon. The entrainment of the reworked Archean parautochthon under the APB generated a duplex thrust sheet, which resulted in the consequent northwestward thrusting of the reworked Archean parautochthon over the pristine Archean terrane. Finally, the ABT was offset by post-Grenvillian normal faulting associated with Ottawa-Bonnechere graben.

ACKNOWLEDGEMENTS

I would first like to thank my supervisor, Alan Dickin, for suggesting the research topic and for being a great advisor. His help and advise along the way was appreciated and his letting me tackle this project allowed me to enjoy many gneiss dates. An extended thanks goes to Bill Morris for his teaching and help in the geophysics lab. I would like to thank all of my friends in and out of the School of Geography and Geology; especially Sara Deschamps for insightful talks about hard rocks, Chris Drielsma for his help in the field and also Matt Pozza and Kristi Markham for showing me some tricks of the trade when operating geophysical software. My office mates Feride Serefiddin and Brad Markham (¿Qué?) are also thanked for their endless sense of humour and for keeping stress levels in the office to a minimum. I would also like to thank my wife Elisa, for supporting me financially and keeping me sane during my tenure as a graduate student. I appreciate the help of my family who have always been there for me and mi familia política que ha estado siempre con nosotros a pesar de estar muy lejos de aquí.

TABLE OF CONTENTS

LIST OF FIGURES

LIST OF TABLES

CHAPTER 1

THE GRENVILLE PROVINCE

1.1 Introduction

The Grenville Province is an ancient orogenic belt, which forms the southeastern margin of the present day Canadian Shield. It represents an area that was once an active continental margin where new continental crust was intruded or sutured to the ancient continent Laurentia for almost a billion years until it was terminated by the uplift of the Grenville Orogeny at approximately 1.1 Ga. The majority of the province is located in southeastern Canada, outcropping as far west as Georgian Bay, Ontario and extending to the Atlantic coast in the east (Figure 1.1). The northwestern limit of the Grenville Province is truncated by the Archean aged Superior Province and to the southeast it is overlain by Paleozoic sediments.

The Grenville Province was formed in a continent-continent collision similar to the Himalayas (Easton, 1988; Easton, 1992) and resulted in major shortening and thickening of the continental crust. This metamorphic event essentially “erased” much of the history of the Grenville Province, making it geologically difficult to interpret. Although many authors have reviewed the evolution of the province (e.g. Easton, 1986; Hoffman, 1989; Rivers et al., 1989, Davidson, 1998), our understanding of its formation is still limited and constantly changing.

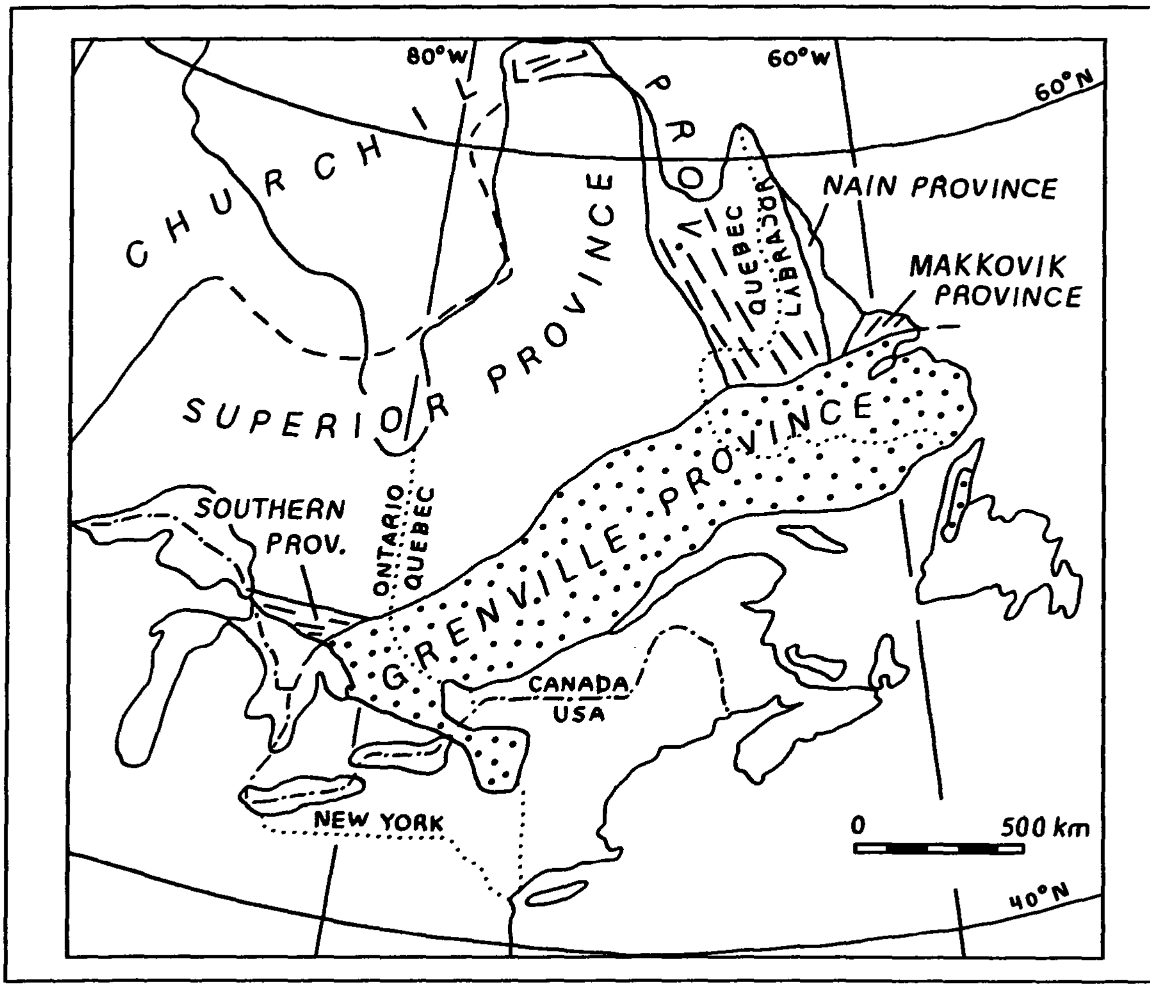

Figure 1.1: Geographic Location of the Grenville Province. Modified from Rivers et al. (1989).

1.2 Structural Studies of the Grenville Province

Studies of the Grenville Province began at least as early as the mid-nineteenth century (Logan, 1847), but it was Wynne-Edwards (1972) who first divided the province into lithotectonic domains that are still, in part, recognized today. He demarcated the province into the following seven segments: the Grenvillian Foreland Belt, the Grenville Front Tectonic Zone, the Central Gneiss Belt, the Central Metasedimentary Belt, the Central Granulite Terrain, the Baie Comeau Segment and the Eastern Grenville Province (Figure 1.2), based on metamorphic character. However, new structural and geochronological studies showed that some regions of the Grenville Province have been subjected to more than one metamorphic event. Therefore, characterizing the province based only on metamorphic differences is not very meaningful when studying orogenies that have evolved with polycyclic histories.

Rivers et al. (1989) established a more fundamental method of dividing the belts of the Grenville Province. Based on geological, geophysical, and geochronological information, Rivers et al. (1989) identified three first-order longitudinal tectonic belts within the province, which are separated by three first-order tectonic boundaries. They are described in Rivers et al. (1989) from northwest to southeast as the Grenville Front, the Parautochthonous Belt, the Allochthon Boundary Thrust, the Allochthonous Polycyclic Belt, the Monocyclic Belt Boundary Zone, and the Allochthonous Monocyclic Belt (Figure 1.3). These divisions form the present day nomenclature of the Grenville Province and each is briefly described as follows.

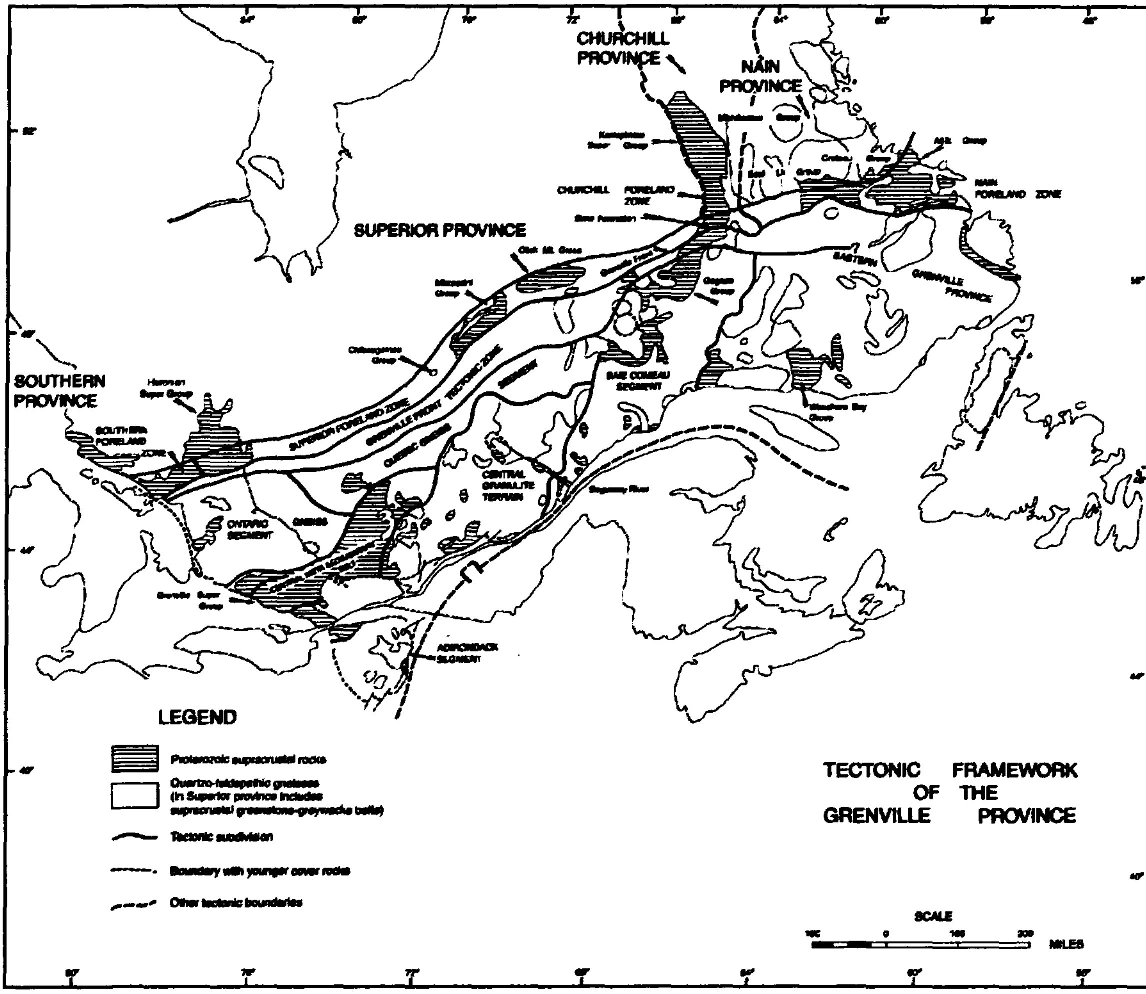

Figure 1.2: Initial tectonic divisions of the Grenville Province. Modified from Wynne-Edwards (1972).

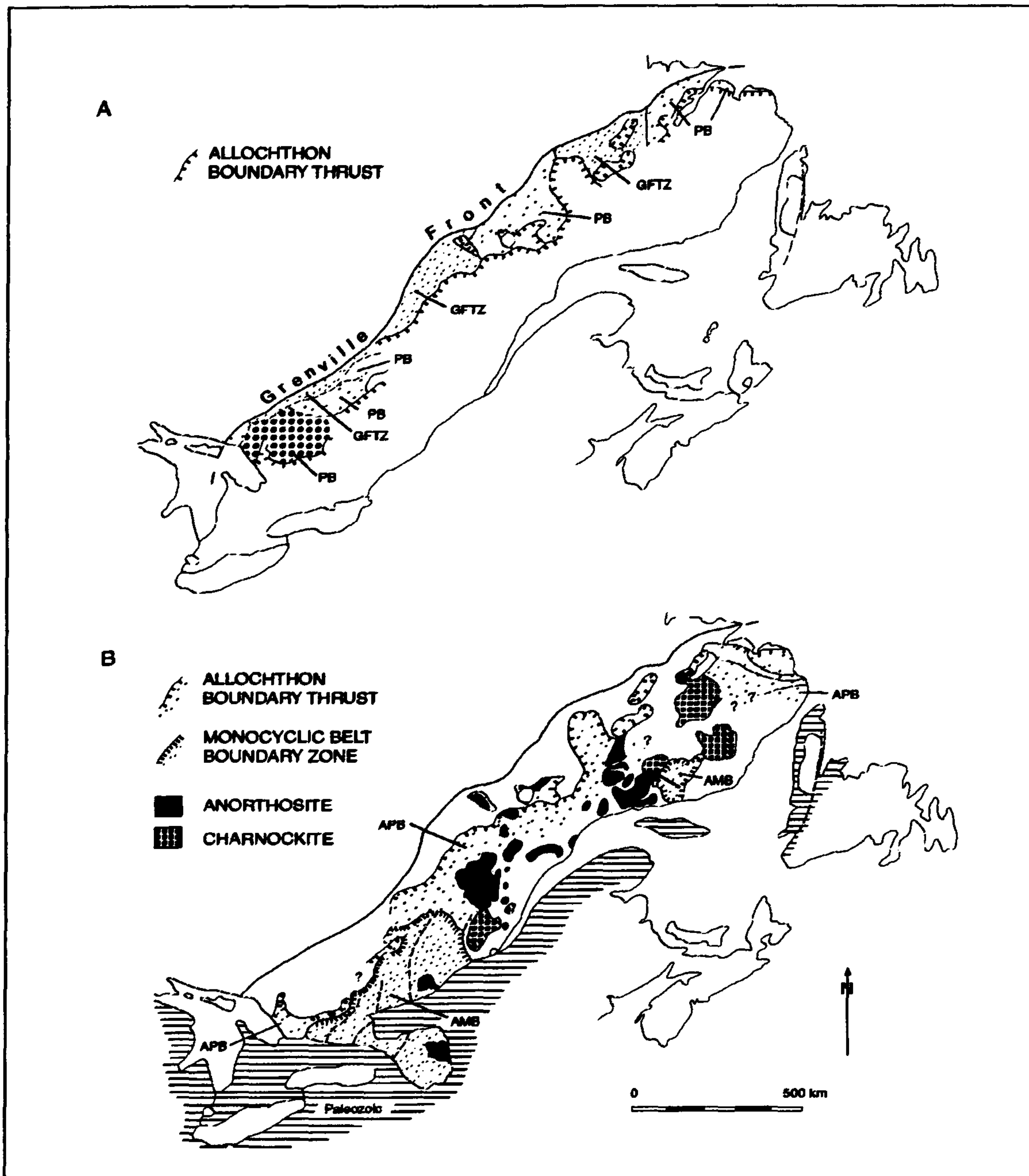

Figure 1.3: The new tectonic divisions of the Grenville Province. Modified from Rivers et al. (1989). Diagram A. illustrates the domains in the parautochthonous belt where PB = Parautochthonous Belt and GFTZ = Grenville Front Tectonic Zone. Diagram B. illustrates the location of the monocyclic (AMB) and polycyclic allochthonous belts (APB). Dense stipple = monocyclic belt; less dense stipple = polycyclic belt.

The Grenville Front is defined as the zone that separates the Archean cratonic provinces from the northwestern portions of the Grenville Province. It is identified by major uplift, a change in metamorphic grade, faulting, mylonitization and defines the limit of regional metamorphism of the Archean cratonic provinces associated with the uplift of the Grenville orogeny. The Parautochthonous Belt (PB) is a first-order longitudinal belt that lies immediately southeast of the Grenville Front and extends up to 150 km southeast, where it is truncated by the Allochthon Boundary Thrust. The PB includes those rocks of the Archean cratonic provinces whose metamorphic lithologies can be attributed to the regional metamorphism associated with the Grenville orogeny. Furthermore, the PB also hosts many second-order lithotectonic terranes that have Archean and Paleoproterozoic affinities but have not undergone large scale lateral transport during the formation of the Grenville.

The Allochthon Boundary Thrust (ABT) is a first-order boundary that separates the PB from the terranes of the Allochthonous Polycyclic Belt to the southeast. The ABT is defined as the limit of major crustal transport towards the northwest, and also marks a break in radiogenic isotopic ages. The rocks in the footwall of the thrust zone (PB) are generally defined by Archean to Paleoproterozoic ages, whereas rocks in the hanging wall are generally much younger with Mesoproterozoic origins. The hanging wall of the ABT is named the Allochthonous Polycyclic Belt (APB). This belt encompasses all of the area between the ABT and the Monocyclic Belt Boundary Zone and hosts laterally transported second-order lithotectonic terranes, which have undergone at least one other metamorphic event during pre-Grenvillian tectonic collisions. The APB is composed mainly of high-grade metamorphic rocks such as orthogneiss and paragneiss containing younger plutons.

The Monocyclic Belt Boundary Zone (MBBZ) is a first-order tectonic boundary located in the southeastern portions of the Grenville Province. The MBBZ separates the second-order terranes of the APB from the Allochthonous Monocyclic Belt (AMB) which host second-order terranes that have only experienced one metamorphic event during the Grenville orogeny. These terranes are primarily comprised of supracrustal rocks of lavas and sediments, deposited sometime before the termination of the Grenville orogeny. Mapping the extent of the AMB is difficult because it is the most southeastern member of the Grenville Province and it is overlain by Paleozoic sediments.

1.3 Geochronological Studies of the Grenville Province

Many different nuclide systems have been employed to model the history of the Grenville Province. However, due to its long polycyclic history, not all isotopic systems yield accurate results. For example, during metamorphism, K-Ar cooling ages in the Grenville are subjected to system resetting and yield a value ca. 1.0 Ga (Easton, 1986), which date the uplift and cooling of the orogeny and not the age of the rocks. On the other hand, U-Pb crystallization ages have provided more accurate results. For example, in the Central Gneiss Belt of Ontario, a wide range of mid-Proterozoic U-Pb ages have been determined (Culshaw et al., 1991; Corrigan et al., 1994; van Breeman et al., 1986). Many Archean U-Pb ages have also been identified south of the Grenville Front (Krogh, 1989; Krogh et al., 1992; Gariepy et al., 1990). This wide range of U-Pb ages illustrates that the Grenville Province has experienced more than one metamorphic event and is made up of terranes that contain rocks of varied crystallization ages.

Whereas other nuclide systems such as U-Pb calculate the time of igneous crystallisation, Nd-model ages are an estimate of the time when continental crust was extracted from the mantle Therefore, employing the Nd-model age method, the time of the oldest event that a crustal terrane experienced is determined. Nd-model age mapping can provide accurate constraints on terrane boundaries because both Nd and its radiometric parent, Sm, are immobile during metamorphic processes. This alleviates the potential of system resetting where other nuclide systems, such as Rb-Sr and K-Ar are less resistant.

Many studies have successfully employed the Nd model age method to formulate pre-Grenvillian reconstructions (e.g. Dickin and McNutt, 1989; Dickin and Higgins, 1992; Moorbath et al., 1997; Dickin, 2000; Dickin and Guo, 2001). Dickin and McNutt (1989) located a tectonic terrane suture 60 km south of the Grenville Front in Ontario, which separated 2.4-2.7 Ga crust in the northern terrane from crust aged at 1.9 Ga to the south. Although it is has been disputed that the 1.9 Ga age is a mixed age with 2.7 and 1.5 Ga counterparts and not actually a crustal extraction age (DeWolf and Mezger, 1994), U-Pb data suggest otherwise. The 1.7-1.74 Ga U-Pb age of plutonic orthogneisses in the region represents a minimum age for this terrane (Corrigan et al., 1994). Based on the proximity of this age to the age calculated by Dickin and McNutt (1989), the youngest component associated with a mixed age in the region can only be 1.7-1.74 Ga and not 1.5

Ga, indicating that the terrane was an Early Proterozoic allochthonous unit that did not inherit any significant Archean component (Dickin, 1997).

On the basis of Nd-model ages, almost all of the Grenville Province has been divided into accreted arc terranes (Dickin, 2000) within the two first-order longitudinal belts of Rivers et al. (1989). However, in certain areas, the boundaries between the terranes remain the subject of interpretative debate.

1.4 Locating the Allochthon Boundary Thrust

One boundary whose location is much debated is the Allochthon Boundary Thrust (ABT). The ABT marks the northwest limit where the Allochthonous Polycyclic Belt was thrust northwestward over the Parauthochthonous Belt, in the Grenville collisional orogen. Therefore, knowing the exact location of the ABT is fundamental to understanding the Grenville Orogeny.

Other methodologies of discriminating first-order tectonic boundaries within the Grenville Province have been developed. A large portion of the ABT has been traced based on aeromagnetic evidence across the majority of the province. At a smaller scale, aeromagnetic evidence has also been very useful. Based on a residual magnetic field map, North (2001) was able to detect previously mapped features such as the Grenville Front Tectonic Zone, the Pickerel Complex, the Fox Bay orthogneisses and both the Britt and Mann Island plutons.

Different ground-based methodologies have also been developed. In the vicinity of Georgian Bay, Ontario, Ketchum (1994) proposed the newly identified Shawanaga shear zone as a suitable location for the ABT. Following this study, Ketchum and Davidson (2000) noted that in this region the ABT separated two distinctly different metabasic rock types. Based on the assumption that the ABT separates crust containing 1.24 Ga metabasic rocks similar to the Sudbury diabase dikes to the north from crust containing 1.16 Ga coronitic meta-gabbros to the south, Ketchum and Davidson (2000) believe that the location and attitude of the ABT can be mapped by discriminating between these two lithologies.

One of the areas where the ABT has proved hardest to delineate is within the Mattawa area on the Ontario-Quebec border. In the vicinity of Mattawa, Ontario, two locations have been proposed for this boundary (Figure 1.4). Based on their assumption that the ABT separates two distinct metabasic rock types, Ketchum and Davidson (2000) suggested that the boundary is located north of North Bay and then traverses eastward, where it rejoins with the Lac Watson Nappe (thin dashed line in Figure 1.4). However, Dickin and Guo (2000) claim that the methodology of Ketchum and Davidson (2000) is not ideal for locating the ABT in this region since the area hosts allochthonous klippen or erosional windows that may carry metabasic rocks. Consequently, Nd model ages calculated from homogenous orthogneisses (Dickin and Guo, 2000) suggest that the ABT follows the geometry of the Lac Watson Nappe to the south and then reappears in Algonquin Park (white area in Figure 1.5, Area 3) where it then traverses westward towards Georgian Bay.

It is the purpose of the present study to locate and isolate allochthonous klippen within this highly debated area to propose a valid location for the ABT. Crustal formation

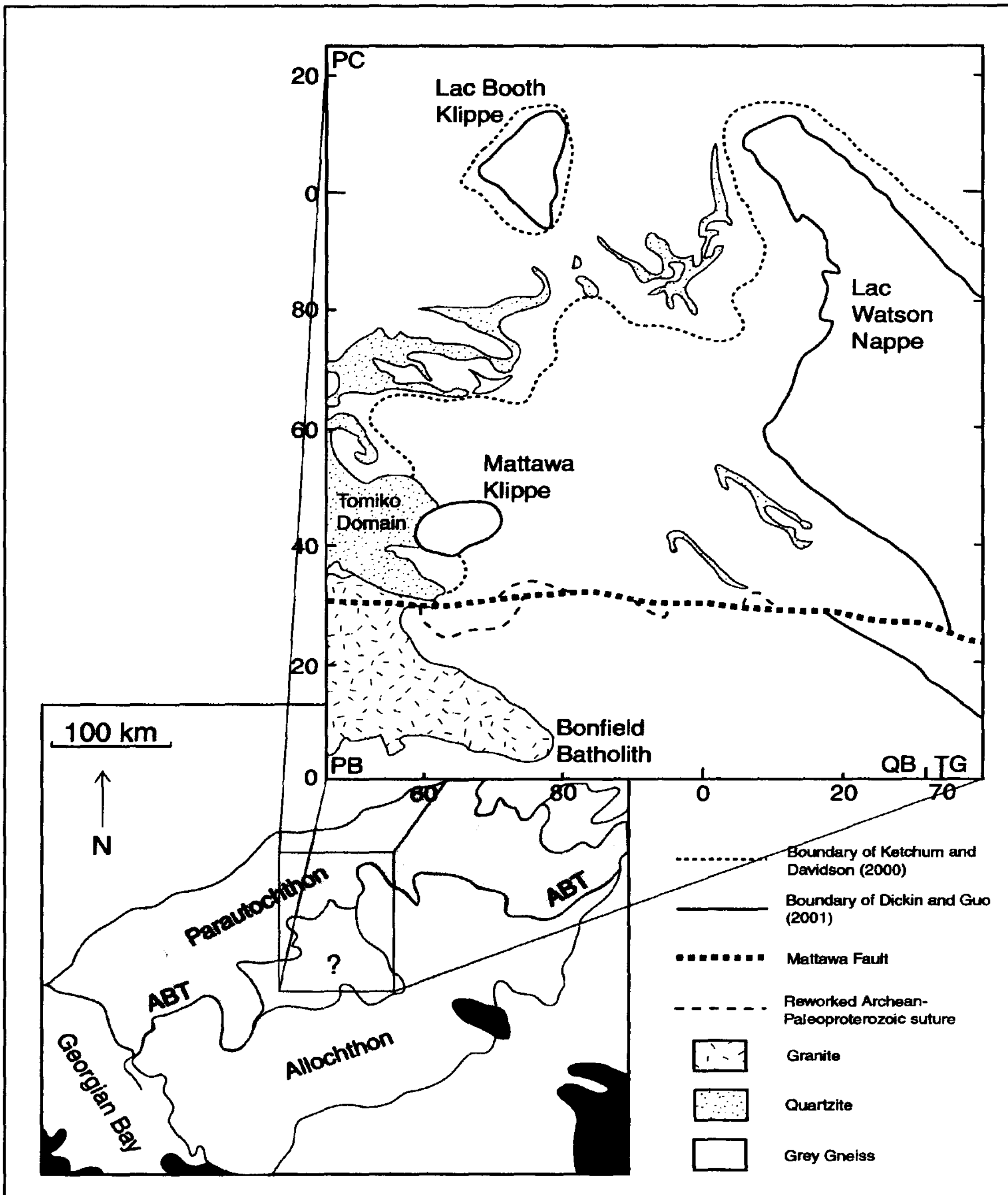

Figure 1.4: Location of the study area showing the two locations of the ABT after Dickin and Guo (2001). Inset modified from Davidson (1998a): Dark shading = parautochthon; pale shading = allochthonous polycyclic belt; white = allochthonous monocyclic belt; black = Paleozoic sediments.

ages will be calculated on samples of homogenous orthogneiss from mainly two different localities. A dense coverage of samples will be analysed northeast of Mattawa to further constrain the boundaries of the formerly identified Mattawa klippe (Dickin and Guo, 2000) and to determine if the 1.16 Ga coronitic metagabbros that Ketchum and Davidson (2000) used to map the ABT are contained within the klippe. This will provide constraints on the methodology that is to be employed when mapping and interpreting highly metamorphosed and deeply exhumed orogenic belts. Reconnaissance scale mapping will also be employed in the Algonquia terrane to locate and determine the direction of the ABT south of the Mattawa fault. To provide further constraints on the radiometric boundaries, aeromagnetic data will be extracted from the province wide compilation of the OGS (1993) to produce a residual magnetic field map. This dataset will be interpreted structurally to interpolate between isotopic data points. Determining the location of the ABT within this highly debated area will provide valuable information about the evolution of this region and will allow detailed structural studies of the ABT.

1.5 Geological Context of the Field Area

The field area is illustrated in Figure 1.4. It encompasses a rectangular area of approximately 10,000 km^2 extending from 45° 15′ N, 79° 30′ W in Ontario to 47° 15′ N, 77° 30′ W in Quebec. Throughout the entire field area, the basement lithologies are dominated by high-grade metamorphic rocks such as orthogneiss and paragneiss whose precursors have been subjected to granulite to upper amphibolite grade metamorphism.

Likewise, large masses of quartzite are present dispersed in various locations (Figure 1.4). Based on major element analyses (Dickin and Guo, 2001), the precursor rocks are a mixture of the different granitoid lithologies of the TTG (tonalite, trondjemite, granodiorite) association with fewer occurrences of syenite, quartz syenite and quartz diorite. However, many of these basement rocks are overlain by Quaternary glacial deposits and dense vegetation, and only outcrop at small scales, making sampling difficult.

Within this area three separate sub-areas were chosen as sampling localities based on previous Nd-model age mapping (Martin, 1992; Dickin and Guo, 2001) and the geological maps of Ontario (Lumbers, 1976) and Quebec (Lyall, 1959; Sabourin, 1960; Rive, 1973a,b). The first sub-area is located in the northern part of the study area (Figure 1.5) and includes most of the Quebec portion of the field area. Samples in this region were collected from both the PB and the APB to investigate the boundary between Archean crust and early Proterozoic crust and also from the Lac Booth klippe and the Lac Watson nappe to examine the presence of a duplex under the allochthon.

The second sub-division is centered around Mattawa, Ontario (Figure 1.5). This is the location of the previously identified allochthonous Mattawa klippe (Dickin and Guo, 2001). A dense distribution of samples was collected in this region for two reasons. First to determine the extent and geometry of the Mattawa klippe and secondly, to determine if the klippe hosts the 1.16 Ga coronitic meta-gabbros that Ketchum and Davidson (2000) identified to trace the location of the ABT. If present, this will have implications on their model since Nd-model ages (Dickin and Guo, 2001) have indicated that this unit is a

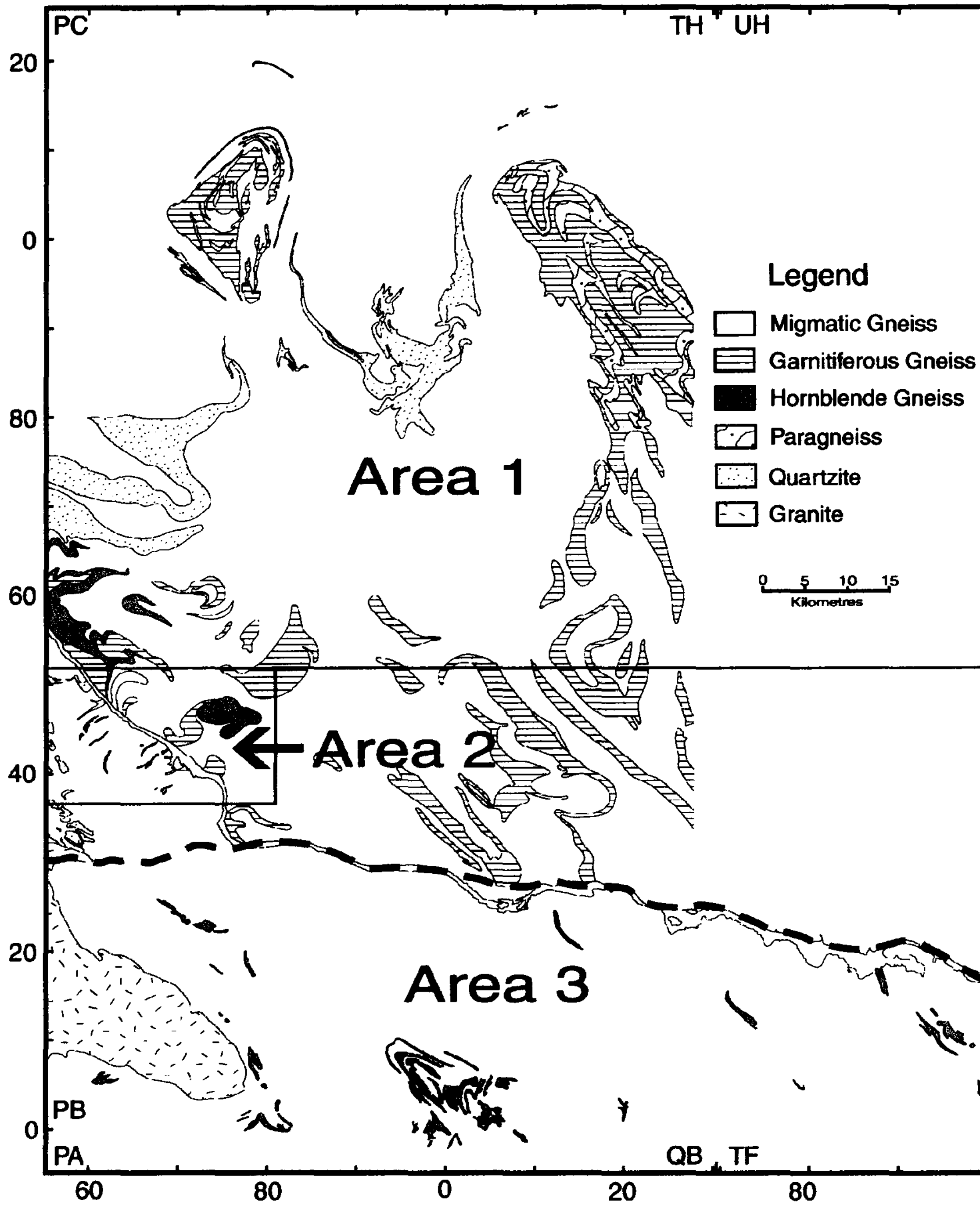

Figure 1.5: Geographical location of the three different field sub-areas.

remnant of the APB, indicating that the actual location of the ABT is further south. Therefore, the methodology of Ketchum and Davidson (2000) for locating the ABT could be rendered less meaningful in geologically complex regions.

The final sampling sub-area is located further south (Figure 1.5) around the north perimeter of Algonquin Park, Ontario. In this locality, only reconnaissance scale mapping has been performed (Martin, 1992) and the exact location and geometry of the ABT is still unknown. Here a denser distribution of samples were collected to further constrain the location of the ABT, however, due to the lack of outcrop and logging roads, the present work in this area can still, at most, be considered reconnaissance.

Detailed mapping in the regions discussed above is essential to determine one of the last misunderstood locations of the ABT. Likewise, it will provide useful constraints on methodologies that are to be used when mapping geologically complex regions.

CHAPTER 2

SM-ND ISOTOPE SYSTEMATICS

The Earth formed 4.6 billion years ago and continental material has been formed by subsequent "melting off" of lighter elements from the mantle. This newly derived continental material remains buoyant over the mantle as a result of its lighter density; however, a fraction of this material may be re-incorporated into the mantle as a result of subduction. The portion that remains buoyant forms terrestrial microcontinents, which over time can collide to form larger macrocontinents. In the context of the Grenville Province, many of the boundaries that formed as a result of microcontinental collisions are obscured as a result of metamorphism associated with the Grenville orogeny. Therefore, it is essential to utilize a radiometric dating system that is capable of yielding crustal extraction ages when formulating pre-Grenvillian evolution models.

One suitable method for calculating crustal extraction ages in metamorphosed terranes is by the Sm-Nd isotopic system, due to the chemical immobility of these elements in geological processes (Dickin, 1995). According to the law of radioactive decay, employing the Sm-Nd system, the age of a rock can be calculated from the following formula:

$$^{143}\mathrm{Nd}/^{144}\mathrm{Nd} = (^{143}\mathrm{Nd}/^{144}\mathrm{Nd})_I + {}^{147}\mathrm{Sm}/^{144}\mathrm{Nd}\,(e^{\lambda t} - 1)$$

Where: λ = radiometric decay constant
t = time in years

The following three parameters are needed to satisfy the equation. The present day isotopic ratios of $^{143}Nd/^{144}Nd$ and $^{147}Sm/^{144}Nd$ and the initial isotopic ratio of $^{143}Nd/^{144}Nd$. The present day isotopic ratios can be measured by conventional mass spectrometry, but the initial ratio of $^{143}Nd/^{144}Nd$ must be determined before an age can be calculated. One method of determining this ratio is to plot an isochron line of present day values of $^{143}Nd/^{144}Nd$ vs. $^{147}Sm/^{144}Nd$ for a whole suit of rocks of the same age, where the slope of this line is equal to λt. However, the isochron method requires a large number of samples from each locality and is less cost-effective. It is more cost-effective and time efficient to calculate crustal extraction ages by determining a Nd-model age.

A model age is determined by assuming that the initial $^{143}Nd/^{144}Nd$ ratio of the rock is equal to the $^{143}Nd/^{144}Nd$ ratio of the mantle at the time it was extracted (Arndt and Goldstein, 1987; Nelson and DePaolo, 1985). Originally, the Chondritic Uniform Reservoir (T_{CHUR}) model of DePaolo and Wasserburg (1976) was used where terrestrial igneous rock ages and their respective initial $^{143}Nd/^{144}Nd$ compositions illustrated a direct correlation to the Chondritic Uniform Reservoir (CHUR) evolution line determined from meteorites (Figure 2.1). Noticing this correlation, DePaolo and Wasserburg (1976) concluded that if the CHUR evolution line represents the initial ratios of terrestrial igneous rocks, knowing the present day values of $^{143}Nd/^{144}Nd$ and $^{147}Sm/^{144}Nd$, one could determine the age of any rock sample from the following formula:

$$T_{CHUR} = \frac{1}{\lambda} \cdot \ln\left[1 + \frac{\left(\frac{^{143}Nd}{^{144}Nd}\right)^0_{sample} - \left(\frac{^{143}Nd}{^{144}Nd}\right)^0_{CHUR}}{\left(\frac{^{147}Sm}{^{144}Nd}\right)^0_{sample} - \left(\frac{^{147}Sm}{^{144}Nd}\right)^0_{CHUR}}\right]$$

However, deviations between the $^{143}Nd/^{144}Nd$ initial isotopic ratios of the samples and the CHUR composition become increasingly large for rocks of younger age (MORB in Figure 2.1) (DePaolo, 1981). Therefore, rocks with younger crustal extraction ages calculated based on the T_{CHUR} model are likely underestimated.

To alleviate this problem, DePaolo (1981) postulated that younger mantle-derived material must have evolved from a depleted mantle source. In his study with Wasserburg (1976), a method for representing deviations from CHUR was developed by normalizing all initial $^{143}Nd/^{144}Nd$ isotopic ratios to CHUR from the following formula:

$$\in Nd(t) = \left[\frac{(^{143}Nd/^{144}Nd)_{sample}(t)}{(^{143}Nd/^{144}Nd)_{CHUR}(t)} - 1\right] \times 10^4$$

DePaolo (1981) noticed that rocks that were younger than 2.7 Ga began to deviate from the CHUR evolution line and concluded that the T_{CHUR} model was only representative of crustal extraction ages greater than 2.7 Ga. Likewise, isotopic measurements on mid-ocean ridge basalts (MORB) (DePaolo and Wasserburg, 1976) corresponded to epsilon-Nd values of +7 to +12, indicating that the mantle has not evolved along the same evolution line of CHUR. Thus DePaolo (1981) concluded that

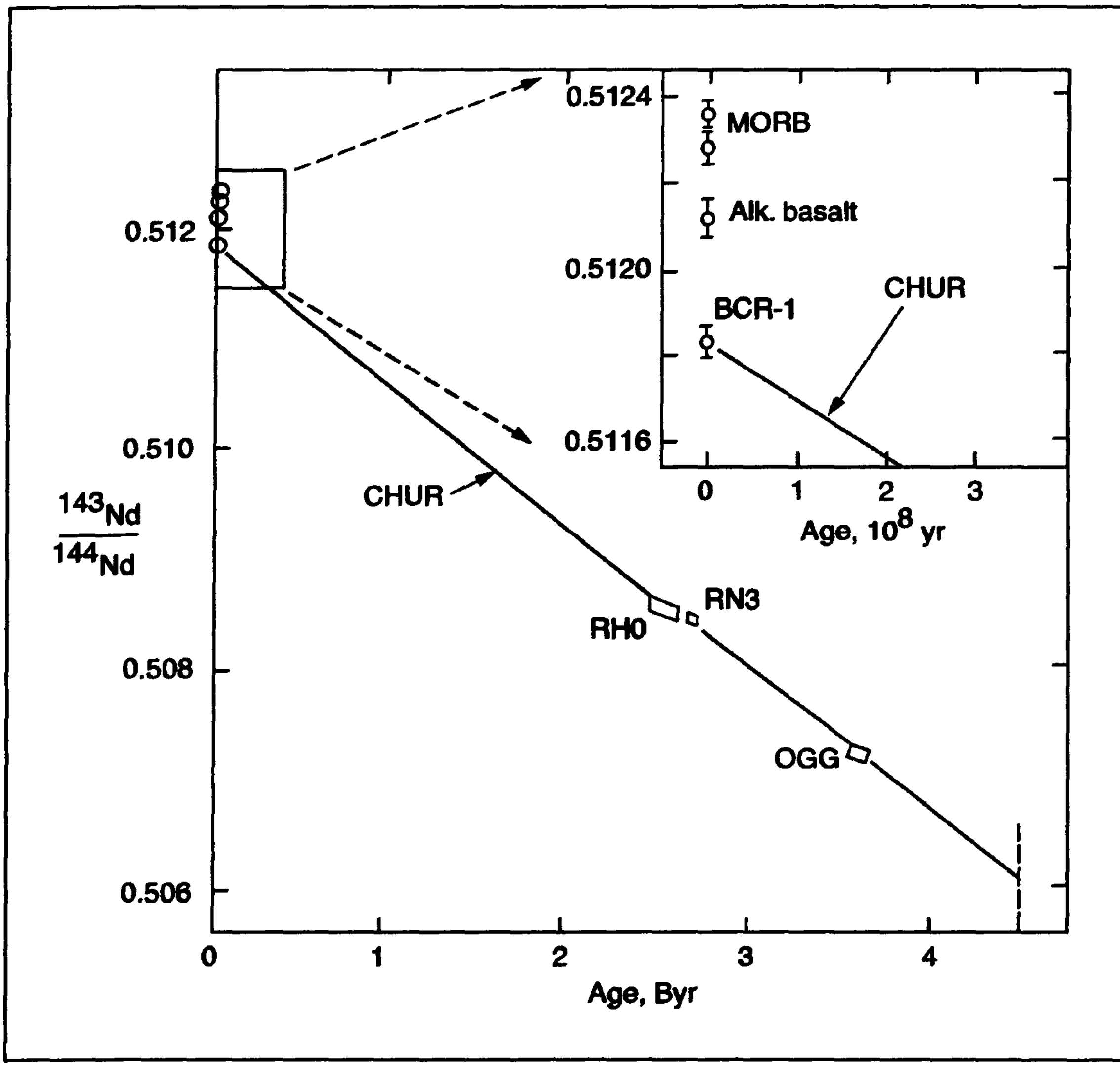

Figure 2.1: Chondritic Uniform Reservoir (CHUR) evolution curve after DePaolo and Wasserburg (1976).

when the mantle melts during crustal extraction processes, Sm and Nd fractionate, enriching the magma in Nd.

The continual extraction of crustal material through time has led to a depletion in the Nd composition of the mantle so that terrestrial igneous rocks younger than 2.7 Ga have been derived from a depleted mantle source.

Based on crustal extraction ages of mantle derived material from the Colorado Front Range and MORB (representing present day mantle derived material), DePaolo (1981) generated a curve through these sample compositions up to present time, creating an evolution curve for the depleted mantle that continually diverges away from the CHUR evolution line with time (Figure 2.2). Mathematically, the evolution curve of a depleted mantle source can be represented as a quadratic in the following formula:

$$\varepsilon \text{ Nd } (T) = 0.25T^2 - 3T + 8.5$$

By measuring the present day isotopic ratios of $^{143}Nd/^{144}Nd$ and $^{147}Sm/^{144}Nd$ a present day epsilon-Nd value can be calculated. The $^{147}Sm/^{144}Nd$ ratio of the rock can then be used to calculate an evolution line for the rock (Labelled "Crust" in Figure 2.2). The point at which this line intersects the evolution curve of the depleted mantle is the time of crustal extraction of that rock from a depleted mantle source.

Nd-model ages allow identification of different tectonic boundaries in highly metamorphosed terranes. However, Arndt and Goldstein (1987) state when using such a model the following assumptions must be considered: 1) The isotopic evolution of the depleted mantle source is correct, 2) The mantle extraction time is relatively short so that the initial $^{143}Nd/^{144}Nd$ ratio of the continental crust equals the $^{143}Nd/^{144}Nd$ ratio of the

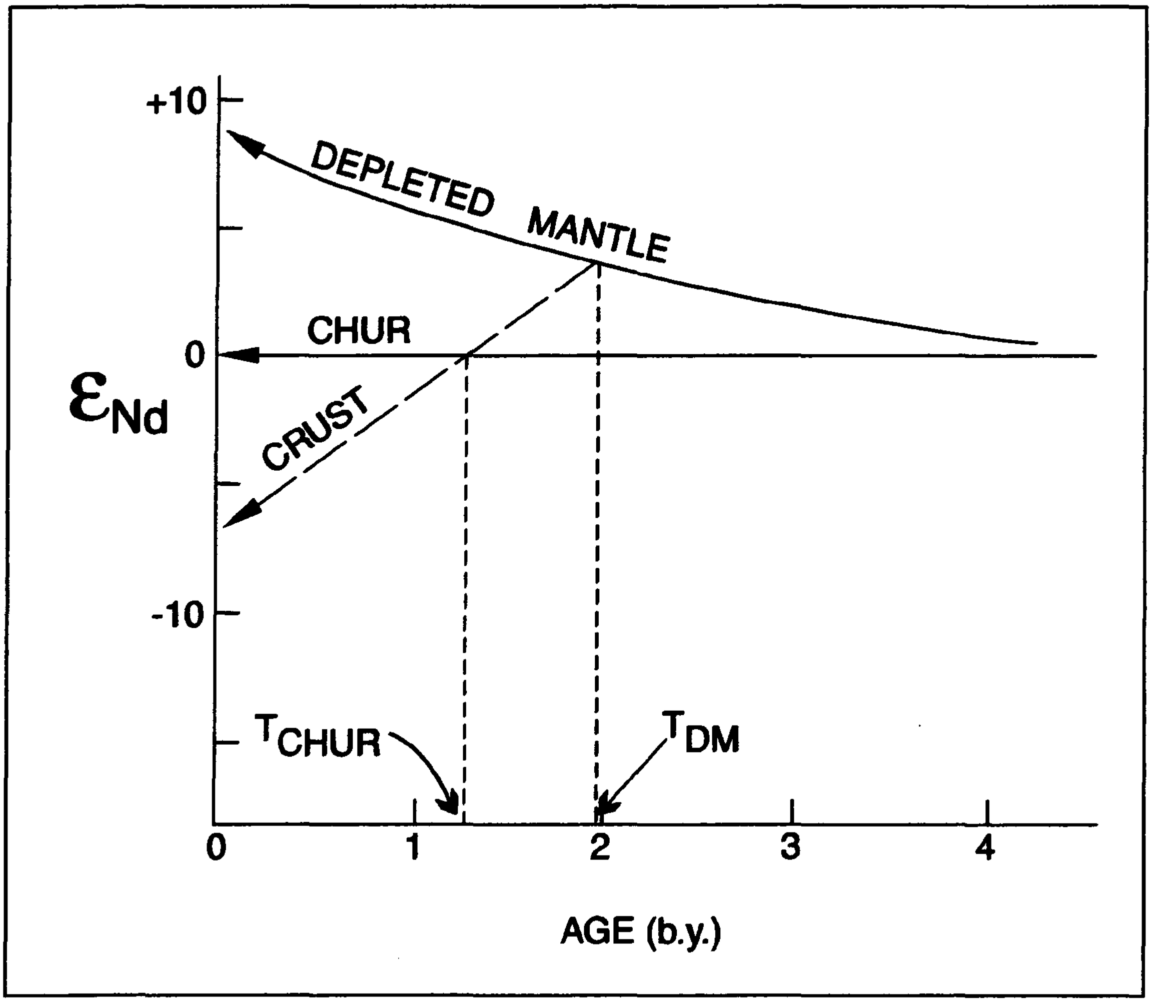

Figure 2.2: Depleted mantle evolution curve after DePaolo (1981a).

mantle at that time, and 3) The Sm-Nd isotopic ratio has not been altered by terrestrial processes such as metamorphism and sedimentation.

Dickin and Higgins (1992) considered these assumptions and validated the depleted Nd-model by matching depleted mantle model ages (T_{DM}) with crustal extraction ages calculated from isochron regression line fitting. Albeit there were minor fluctuations in the ages, the T_{DM} ages were within error of the crustal extraction ages determined from isochron regression lines.

CHAPTER 3

RESULTS: NORTHERN SECTION

3.1 Geological Context

The northern section of the field area encompasses approximately 5000 km^2 extending from 46°30′ N, 79°00′ W in the southwest to 47°15′ N, 78°00′ W in the northeast (Figure 3.1). Based on previous studies (Dickin and Guo, 2001), there are three distinct Nd-model age ranges within the region. Archean units with Nd-model ages greater than 2.6 Ga form part of the parautochthonous belt whereas the limits of allochthonous units are mapped to contain a mixture of Nd-model ages less than 1.8 Ga. The area also hosts an intermittent range of ages from 1.9-2.6 Ga which are the result of mixed ages containing an Archean component, reworked by plutonism and migmatization associated with the Grenville collisional orogeny. Rock units of these ages form the magmatically reworked Archean parautochthon (referred to here as the reworked Archean parautochthon).

Two locations of the allochthon boundary thrust (ABT) have been suggested in this region (see above). Ketchum and Davidson (2000) believe that the ABT travels westward across the field area from the northern extent of the Lac Watson nappe due to the presence of 1.16 Ga coronitic metagabbros. Where metabasic rocks area absent, Ketchum and Davidson (2000) argued that the ABT follows the geometry of the Tomiko domain.

This is a quartzite cratonic sequence believed to be overlying the parautochthon (Easton, 1992).

Dickin and Guo (2001) believe that the ABT is much further south, and that the metabasic units are hosted by allochthonous klippen. Based on Nd-model ages (Dickin and Guo, 2001), two structures have been identified as allochthonous, marking the northeast limit of the ABT. In the east the Lac Watson shear zone identified by Indares and Dunning (1997) separates parauthochthonous crust with Nd-model ages ranging from 1.88-2.57 Ga from the allochthonous Lac Watson nappe with a Nd-model age range of 1.59-1.79 Ga. Based on the distribution of these Nd-model ages, the Lac Watson shear zone was postulated to be the location of the ABT, contrary to the location suggested by Ketchum and Davidson (2000).

In the northwest, another allochthonous unit was identified and termed the Lac Booth klippe (Kellet et al., 1994). The principal workers in this region (e.g. Ketchum and Davidson, 2000; Dickin and Guo, 2001) agree that this is an allochthonous unit, however, they disagree on the extent and geometry of the klippe. Originally, the extent of the klippe was mapped based on Lithoprobe seismic reflection results (Kellet et al., 1994) and the distribution of metabasic rocks in the region (Ketchum and Davidson, 2000). However, Dickin and Guo (2001) argue that the Lac Booth klippe is much smaller than originally mapped, based on pristine and reworked Archean Nd-model ages found within the extents of the boundary defined by Kellet et al. (1994) and Ketchum and Davidson (2000).

It was the objective of the present study to collect samples around both of these allochthonous units to further constrain their boundaries to determine the exact location of the ABT within the region.

3.2 Nd-model age mapping

19 new Nd-model ages were calculated on grey orthogneisses using the depleted mantle model of DePaolo (1981) and combined with those of Dickin and Guo (2001) to locate the position and attitude of the ABT in this region. The distribution of these samples is illustrated in Figure 3.1 and the corresponding isotopic data are listed in Table 3.1. However, only the Nd isotopic data for the samples analysed in this study are plotted in Figures 3.2 and 3.3.

Figure 3.2 is an isochron plot of $^{143}Nd/^{144}Nd$ versus $^{147}Sm/^{144}Nd$ which illustrates a geochemical discrimination of the samples into three fields. Two reference lines are also included in this diagram. A 2.7 Ga reference line typical of Archean aged rocks, and a 1.7 Ga reference line representing mid-Proterozoic allochthonous units are shown. It is seen that the Archean aged samples (solid squares) in this study lie on the 2.7 Ga reference line and that the mid-Proterozoic aged samples (solid triangles) cluster around the 1.7 Ga reference line. Reworked Archean samples (solid diamonds) lie in between the two fields with less reworked units closer to the 2.7 Ga reference line.

Figure 3.3 is a plot of epsilon-Nd versus concentration at 1450 Ma. Here it is also seen that the samples can be discriminated into three fields. Rocks with T_{DM} model ages of 2.6-2.9 Ga have relatively low epsilon-Nd and Nd concentrations whereas samples

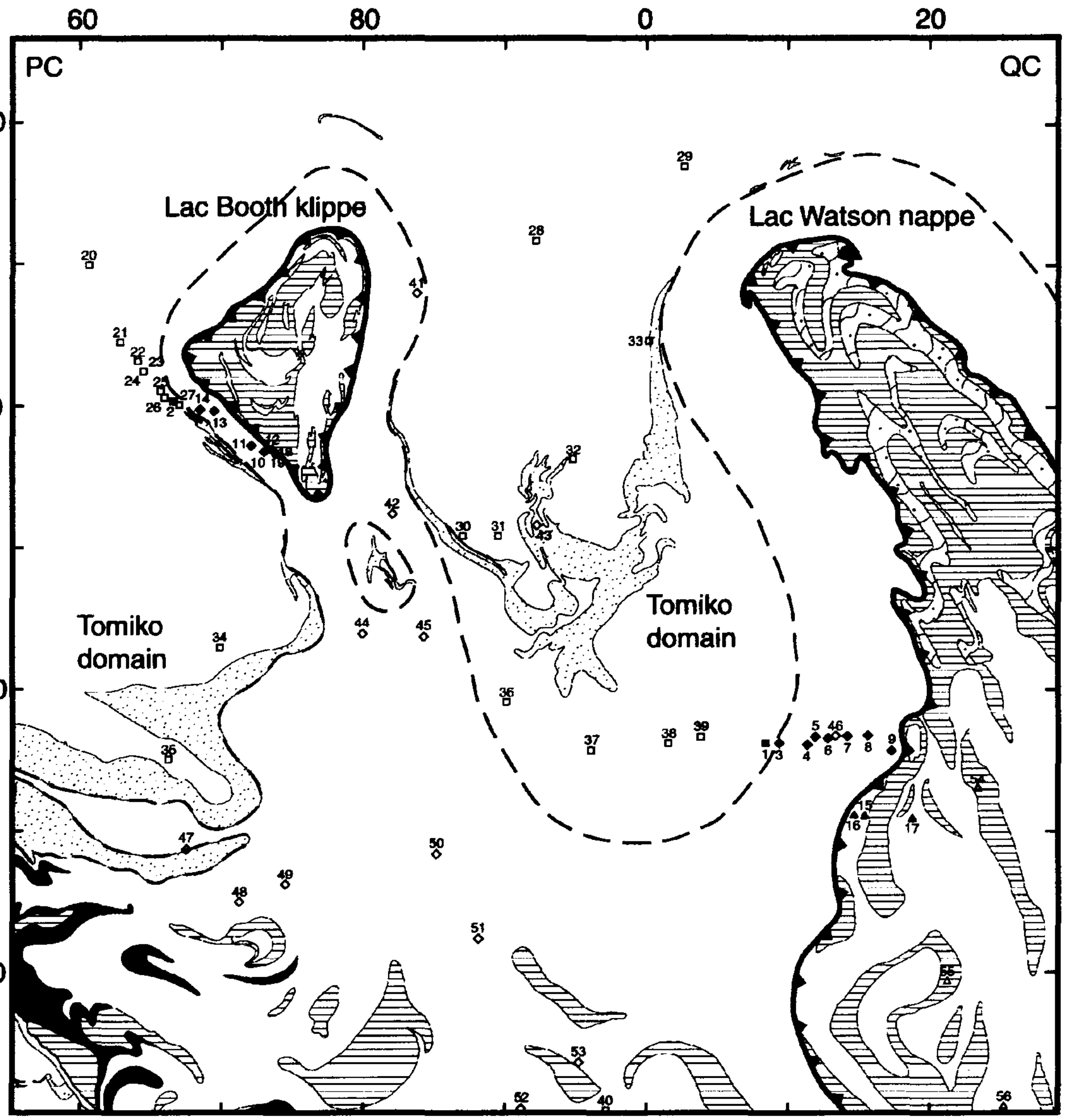

Figure 3.1: Geographical distribution of Nd-model ages illustrating the location of the ABT in the northern region of the study area. Axis labels = 10 km UTM grid squares. Closed squares = Archean parautochthon; closed diamonds = reworked Archean parautochthon; closed triangles = mid-Proterozoic allochthon. Open symbols are the Nd-model age sample locations of Dickin and Guo (2001). Thick dashed line = new boundary separating the Archean and the reworked Archean parautochthons.

Table 3.1: Sm-Nd Isotopic data for the Northern Section of the Study Area

Sample	Grid Reference	Nd ppm	Sm ppm	$^{147}Sm/^{144}Nd$	$^{143}Nd/^{144}Nd$	eNd 1450	T_{DM} (Ga)
New Data							
Archean parautochthon: TDM ages 2.6-2.9 Ga							
1 LF 1	QB 083 770	24.69	4.311	0.1055	0.511124	-12.6	2.72
2 ZK 8	PN 675 002	18.09	3.594	0.1201	0.511415	-9.7	2.67
Reworked Archean parautochthon: TDM ages 1.9-2.6 Ga							
3 LF 2	QB 097 768	53.64	9.757	0.1100	0.511711	-2.0	1.96
4 LF 3a	QB 119 764	62.08	11.108	0.1082	0.511374	-1.5	1.92
5 LF 7	QB 123 767	54.13	9.849	0.1100	0.511694	-2.3	1.98
6 LF 8	QB 134 767	46.93	8.168	0.1052	0.511623	-2.8	1.99
7 LF 9	QB 143 766	55.78	9.189	0.0996	0.511623	-1.7	1.89
8 LF 10	QB 164 766	40.40	7.153	0.1070	0.511672	-2.2	1.96
9 LF 11	QB 180 760	74.29	14.582	0.1186	0.511895	0.0	1.83
10 ZK 1	PM 734 967	51.85	9.667	0.1127	0.511706	-2.6	2.02
11 ZK 2	PM 728 975	54.09	9.380	0.1048	0.511636	-2.5	1.97
12 ZK 3	PM 739 967	34.38	6.073	0.1068	0.511683	-1.9	1.94
13 ZK 6	PM 701 998	46.96	9.484	0.1221	0.511905	-0.4	1.89
14 ZK 7	PN 689 000	33.78	5.974	0.1069	0.511405	-7.4	2.34
Lac Watson nappe: TDM ages <1.8 Ga							
15 LF 4*	QB 161 714	34.44	5.766	0.1012	0.511933	4.0	1.50
16 LF 5	QB 158 710	44.26	7.405	0.1011	0.511753	0.5	1.74
17 LF 6	QB 184 715	54.14	9.932	0.1109	0.511951	2.6	1.61
Lac Booth klippe: TDM ages <1.8 Ga							
18 ZK 4	PM 741 965	19.76	4.851	0.1484	0.512449	5.3	1.38
19 ZK 5	PM 741 963	36.82	5.728	0.0940	0.511697	0.7	1.71
Published Data (Dickin and Guo, 2001)							
Archean parautochthon: TDM ages 2.6-2.9 Ga							
20 KP 1	PC 605 102	17.77	2.75	0.0934	0.510954	-10.4	2.66
21 KP 3	PC 627 047	10.67	2.16	0.1224	0.511455	-6.9	2.67
22 KP 5	PC 643 031	21.90	3.37	0.0930	0.510945	-10.5	2.67
23 KP 6	PC 645 028	26.24	3.98	0.0916	0.510904	-11.0	2.69
24 KP 7	PC 645 029	4.52	0.949	0.1269	0.511424	-8.5	2.88
25 KP 11	PC 657 014	15.76	2.51	0.0964	0.510985	-10.4	2.69
26 KP 12	PC 659 009	12.01	2.39	0.1204	0.511395	-7.7	2.72

Sample	Grid Reference	Nd ppm	Sm ppm	$^{147}Sm/^{144}Nd$	$^{143}Nd/^{144}Nd$	eNd 1450	T_{DM} (Ga)
27 KP 10	PC 668 003	25.24	4.55	0.1089	0.511192	-9.1	2.71
28 GA 8	PC 924 118	3.56	0.51	0.0890	0.510892	-10.6	2.64
29 GA 9	QC 025 170	10.92	2.17	0.1216	0.511478	-6.3	2.61
30 GA 13	PB 869 909	7.60	1.53	0.1216	0.511393	-8.0	2.76
31 GA 19	PB 895 911	9.04	1.62	0.1083	0.511241	-8.0	2.62
32 GA 17	PB 948 962	1.67	0.33	0.1200	0.511455	-6.4	2.60
33 GA 14	QC 003 046	7.69	1.57	0.1245	0.511481	-6.9	2.69
34 NB 65	PB 698 833	6.59	1.38	0.1263	0.511494	-7.0	2.73
35 NB 54	PB 661 749	6.74	1.09	0.0982	0.511077	-9.0	2.61
36 TM 1	PB 900 790	10.70	1.94	0.1096	0.511167	-9.8	2.77
37 TM 3	PB 959 760	19.12	2.55	0.0808	0.510681	-13.0	2.73
38 TM 5	QB 014 762	17.62	2.19	0.0751	0.510608	-13.2	2.69
39 TM 6	QB 037 768	17.44	3.03	0.1051	0.511095	-10.2	2.75
40 DR 18	PB 971 497	45.17	7.43	0.0994	0.510926	-12.2	2.85
Reworked Archean parautochton: TDM ages 1.9-2.6 Ga							
41 GA 4	PC 835 083	27.10	4.58	0.1029	0.511187	-7.9	2.57
42 GA 12	PB 820 925	56.46	10.01	0.1072	0.511410	-4.5	2.34
43 GA 18	PB 920 917	44.22	9.16	0.1251	0.511765	-1.4	2.20
44 GA 23	PB 800 841	54.85	8.47	0.0929	0.511270	-4.1	2.24
45 GA 21	PB 843 838	43.30	7.02	0.0980	0.511321	-4.2	2.27
46 TM 7	QB 130 767	75.09	13.22	0.1064	0.511658	0.6	1.97
47 NB 51	PB 672 687	75.19	13.66	0.1098	0.511690	0.4	1.98
48 NB 52	PB 714 652	3.07	0.49	0.0965	0.511202	-6.2	2.40
49 NB 53	PB 745 662	17.91	2.61	0.0819	0.510917	-8.6	2.47
50 DR 16	PB 821 669	67.55	10.11	0.0905	0.511132	-6.3	2.37
51 DR 14	PB 880 627	52.99	9.78	0.1116	0.511718	0.6	1.98
52 DR 21	PB 910 502	48.36	9.72	0.1214	0.511819	0.4	2.02
53 DR 12	PB 952 541	43.70	7.06	0.0977	0.511593	-1.2	1.90
Lac Watson nappe: TDM <1.8 Ga							
54 TM 10	QB 234 731	55.65	7.92	0.0861	0.511613	4.1	1.71
55 DR 30	QB 212 597	41.08	8.41	0.1237	0.512102	5.5	1.59
56 DR 28	QB 250 503	32.73	8.30	0.1263	0.512017	3.2	1.79

* Based on average of two dissolutions.
Average error on isotope dilutions was 0.06 % (1σ)
Average error on Nd isotope ratios was 0.010/mil (1σ)

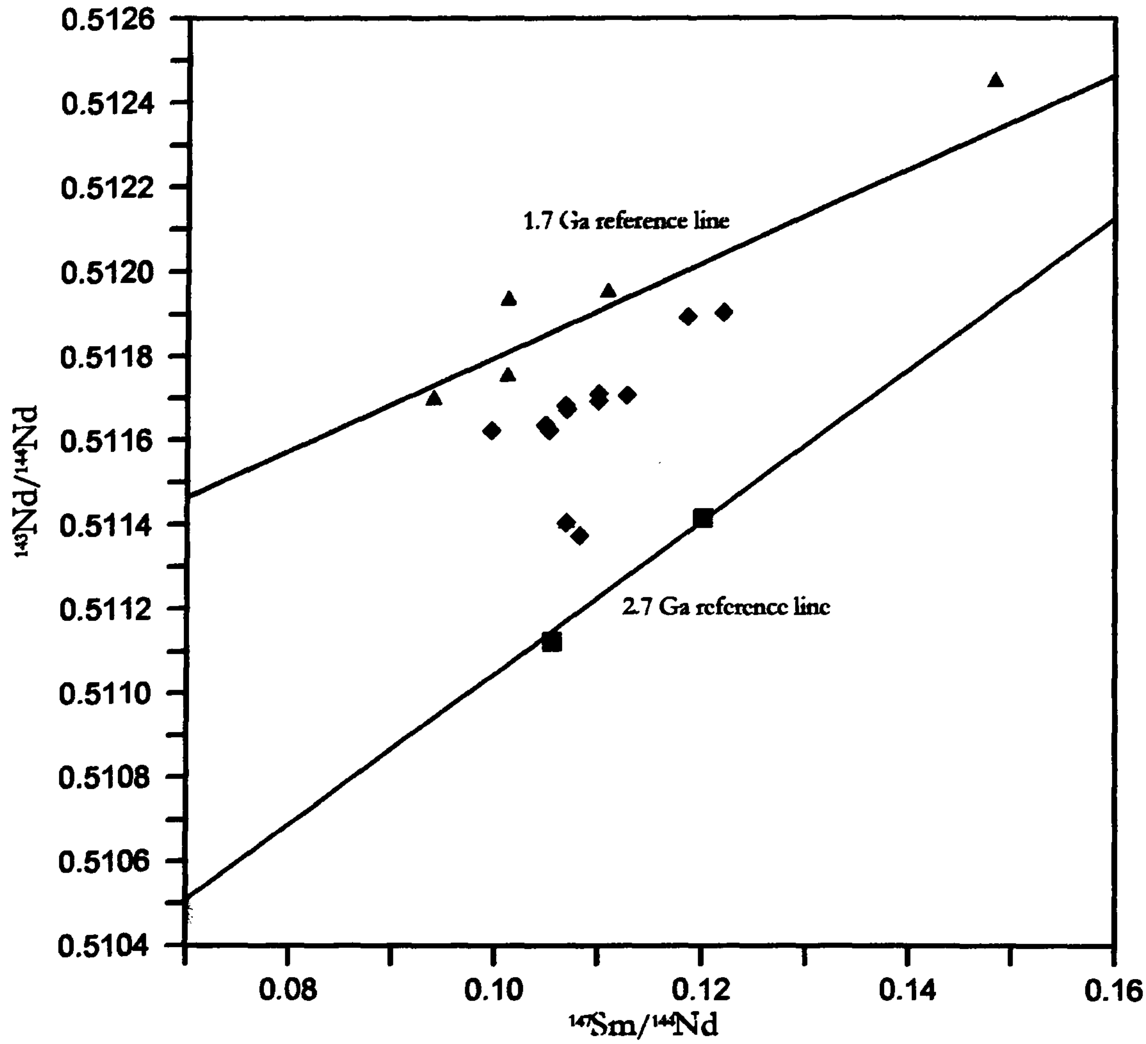

Figure 3.2: Sm-Nd isochron showing geochemical separation of the samples into three fields. Symbols are the same as Figure 3.1.

with T_{DM} ages <1.8 Ga have mixed concentrations but relatively high epsilon-Nd values. The third field is attributed to reworked Archean parautochthonous samples that have an age range of 1.9-2.6 Ga. These samples have a wide concentration range and their epsilon-Nd values are intermediate between mid-Proterozoic allochthonous rocks and Archean parautochthonous rocks.

The large epsilon-Nd range of reworked Archean units indicate the degree to which these samples are reworked. It is seen in figure 3.3 that one reworked Archean sample diverges away from the main cluster towards the Archean parautochthon field (Sample 7). This sample illustrates more of an Archean composition, indicating that it has been reworked to a lesser extent. This sample has a Nd-model age of 2.34 Ga whereas the rocks in the main cluster have a younger average Nd-model age. Therefore, reworked Archean samples that inherit a greater proportion of younger component have compositions further displaced from the Archean parautochthonous field towards the mid-Proterozoic allochthonous field.

When the Nd-model ages are represented geographically (Figure 3.1), it is seen that the three suites discussed above also have a unique distribution. In the east, the Lac Watson shear zone marks a Nd-model age break representing the location of the ABT between mid-Proterozoic allochthonous crust and the reworked Archean parautochthon. Immediately west of the reworked Archean samples, there is also an occurrence of Archean aged crust.

In the northeast, around the Lac Booth klippe, a similar distribution is noticed. Rocks with mid-Proterozoic affinities are exclusively located within the centre of the

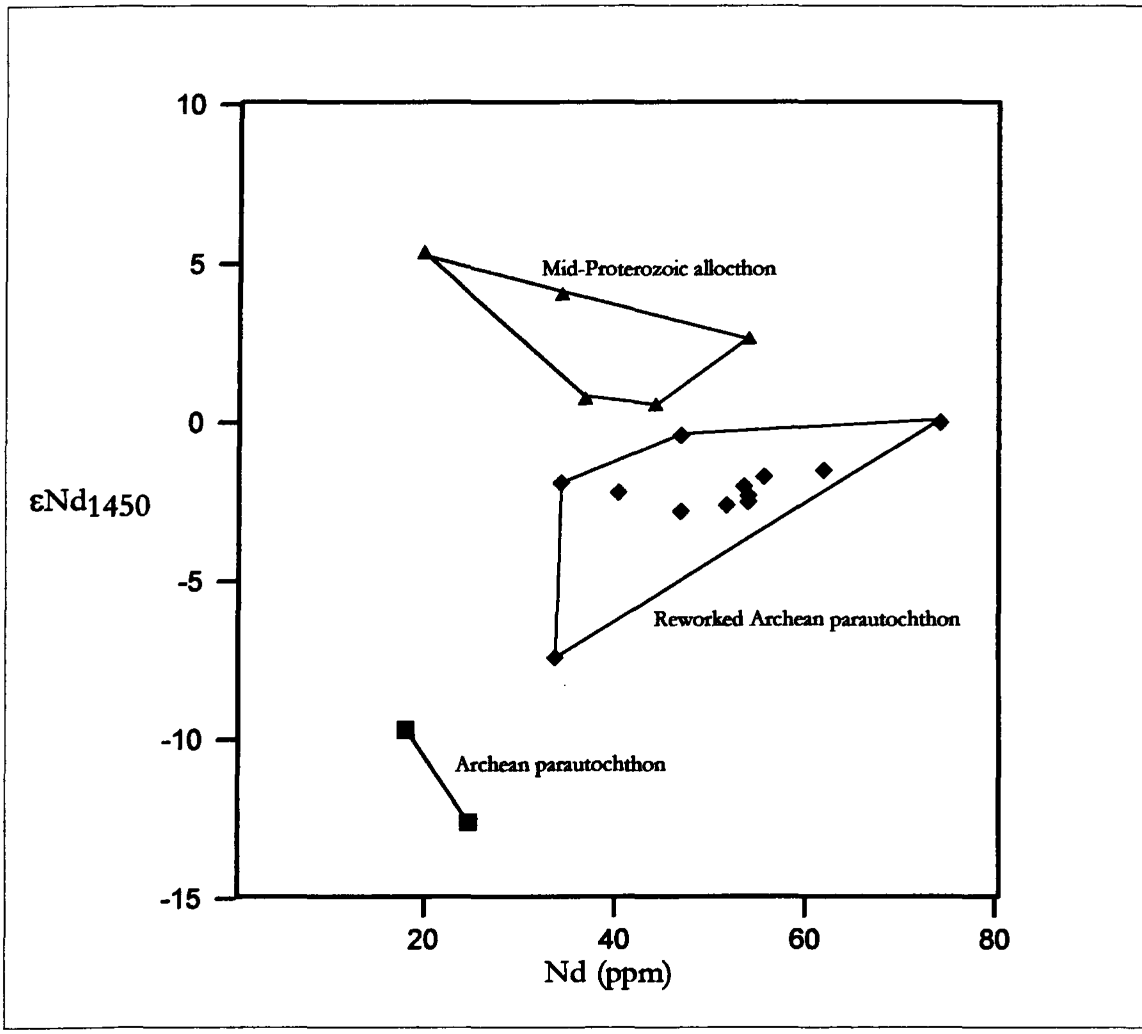

Figure 3.3: Plot of εNd (t) versus concentration. Symbols are the same as Figures 3.1 and 3.2.

structure whereas reworked Archean crust is found around the perimeter of the klippe. Outside this zone, Archean Nd-model ages are also present.

The southern portion of this region near the Ottawa River is a mixture of crust, containing reworked Archean ages with remnant lenses of Archean crust. The presence of these lenses indicates that the intermittent Nd-model age range (1.9-2.6 Ga) is reworked Archean crust that forms part of the Archean parautochthon and is not a separate crustal terrane. Hence an additional model age boundary can be plotted (heavy dashed line in Figure 3.1) separating pristine and reworked Archean crust. This boundary also lies to the southeast of all outcrops of muscovite-quartzite gneiss and can be interpreted as a second thrust fault lying below the main ABT.

The distribution of the Nd-model ages for this region indicates two thrusting events. The presence of Archean Nd-model ages with the absence of a reworked component found in the extreme northwest represent crust that has undergone relatively little deformation. However, further southeast, Archean crustal units are interspersed with reworked Archean crustal units containing various Nd-model ages. This crust is interpreted here as part of the parautochthon that was detached and was thrust northwestward over the Archean parautochthon as a duplex entrained onto the base of the overriding allochthon.

CHAPTER 4

RESULTS: THE MATTAWA KLIPPE

4.1 Geological Context

The Mattawa region of the study area covers a small area of approximately 600 km^2 extending from 46° 22′ N, 79° 00′ W in the southwest to 46° 30′ N, 78° 37′ W in the northeast (Figure 4.1). Similar to the northern portion of the study area, the location of the allochthon boundary thrust (ABT) in the Mattawa region is also disputed. Ketchum and Davidson (2000) proposed that the ABT trends in a north-south direction in this region following the geometry of the Tomiko domain, based on the presence of retrogressed eclogite and 1.16 Ga coronitic metagabbros immediately to the east. The Tomiko Domain is a meta-quartzite unit and was considered to be a Laurentian cratonic sedimentary sequence forming part of the parautochthon (Easton, 1992). However, allochthonous Nd-model ages calculated on rocks east of the Tomiko domain (Dickin and Guo, 2001) were found to be surrounded by crust characterized by reworked Archean parautochthonous ages. Dickin and Guo (2001) concluded that the allochthonous units in this region were confined to a klippe (named the Mattawa klippe) that could host the 1.16 Ga coronitic metagabbros of Ketchum and Davidson (2000). They further concluded that this klippe is an erosional remnant of the allochthonous polycyclic belt (APB) and the main locus of the ABT is located somewhere further south.

Identification of the Mattawa klippe was based solely on two Nd-model ages and the size and geometry of the klippe are uncertain. It was the objective of the present study to collect additional samples in the region to further map the size and the attitude of the Mattawa klippe and to test the tectonic model of Dickin and Guo (2001).

4.2 Nd-model age mapping

30 new Nd-model ages were calculated on grey orthogneisses using the depleted mantle model of DePaolo (1981) and combined with those of Dickin and Guo (2001) to determine the size and exact location of the Mattawa klippe. The geographical distribution of these samples is illustrated in Figure 4.1 and the corresponding isotopic data are listed in Table 4.1. However, only the Nd isotopic data for the samples analysed in this study are plotted in Figures 4.2 and 4.3.

Figure 4.2 is an isochron diagram of $^{143}Nd/^{144}Nd$ versus $^{147}Sm/^{144}Nd$ with 1.7 Ga reference line representing allochthonous units and a 2.7 Ga reference line typical of Archean aged samples. Unlike the samples discussed for the northern section of the study area, the data in the Mattawa region can only be discriminated into two fields. Samples with mid-Proterozoic allochthonous ages cluster around the 1.7 Ga reference line, however, it is seen here that the majority of the units of this affinity lay above this reference line due to their ages being less than 1.7 Ga (Table 4.1). As seen in the northern section of the study area, reworked Archean parautochthonous units are characterized by a large intermediate field located in between the two reference lines illustrating the degree of reworking of each sample.

Figure 4.1: Geographical distribution of Nd-model ages illustrating the location of the ABT in the Mattawa region of the study area. Closed diamonds = reworked Archean parautochthon; closed triangles = mid-Proterozoic allochthon; closed star = retrogressed eclogite. Open symbols are the Nd-model age sample locations of Dickin and Guo (2001).

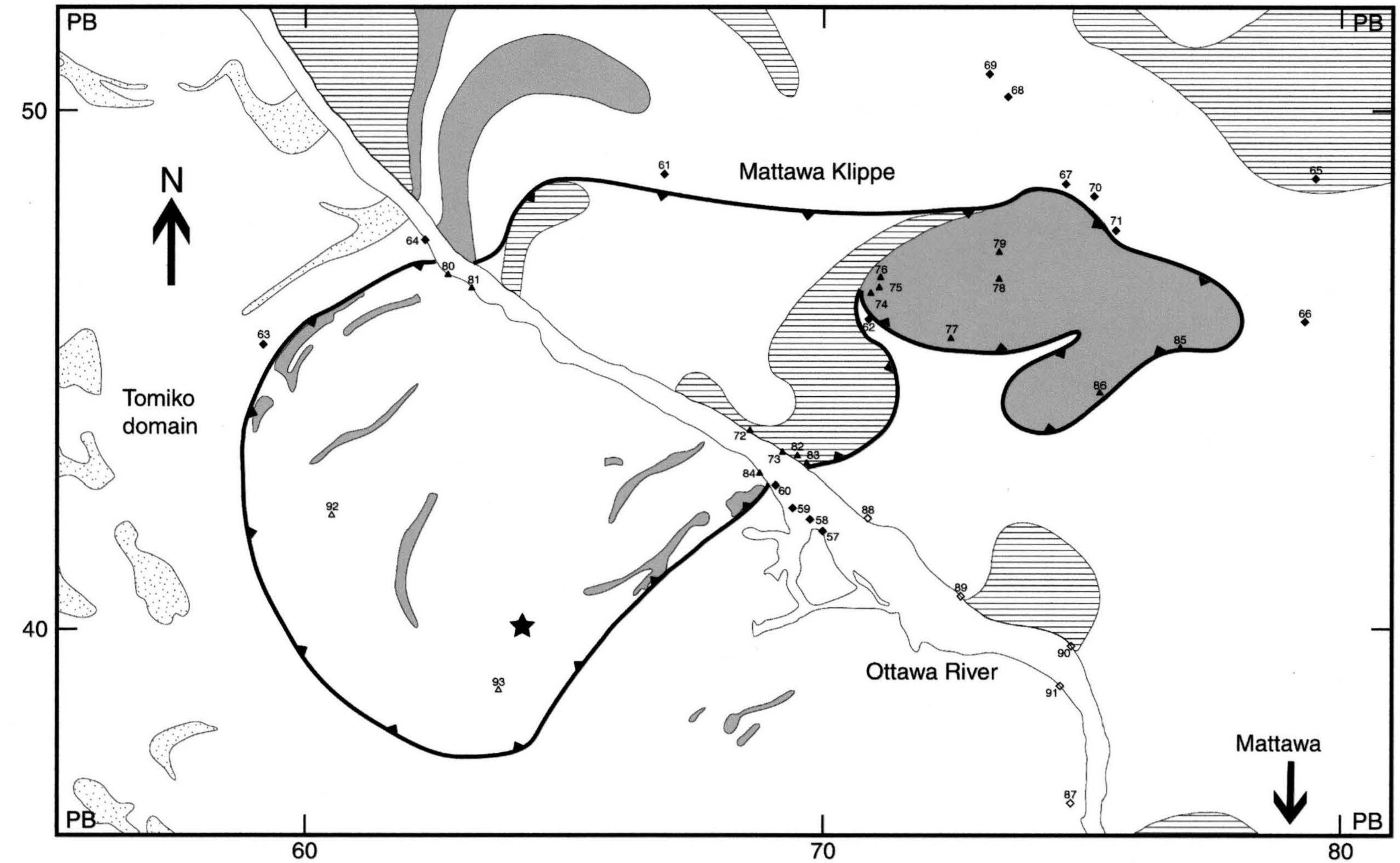
PB
PB
PB
PB
Mattawa Klippe
N
Tomiko
domain
Ottawa River
Mattawa
50
40
60
70
80

Table 4.1: Sm-Nd Isotopic data for the Mattawa Region

Sample	Grid Reference	Nd ppm	Sm ppm	$^{147}Sm/^{144}Nd$	$^{143}Nd/^{144}Nd$	eNd 1450	T_{DM} (Ga)
New Data							
Reworked Archean parautochthon: TDM ages 1.9-2.5 Ga							
57 OR 1	PB 700 419	77.36	12.719	0.09937	0.511497	-4.2	2.06
58 OR 2	PB 697 421	68.99	11.226	0.0984	0.511556	-2.9	1.96
59 OR 3	PB 694 423	83.07	12.472	0.0907	0.511410	-4.3	2.03
60 OR 4	PB 690 427	20.70	3.897	0.1138	0.511752	-1.9	1.97
61 OR 9*	PB 669 487	82.79	14.365	0.1049	0.511634	-2.5	2.10
62 OR 16	PB 707 459	49.68	8.852	0.1077	0.511701	-1.8	1.93
63 OR 24*	PB 591 455	65.00	9.657	0.0898	0.511190	-8.4	2.28
64 OR 26	PB 616 472	59.46	8.575	0.0872	0.511223	-7.3	2.19
65 MW 1	PB 795 487	5.20	0.914	0.1062	0.511313	-9.1	2.46
66 MW 2	PB 792 459	58.58	9.805	0.1012	0.511638	-1.8	1.90
67 MW 6	PB 745 485	31.25	4.794	0.0927	0.511594	-1.1	1.82
68 MW 8	PB 736 502	9.61	1.571	0.0988	0.511221	-9.5	2.43
69 MW 9	PB 732 506	33.34	5.479	0.0993	0.511134	-11.3	2.56
70 MW 10	PB 753 482	20.71	3.638	0.1061	0.511698	-1.5	1.91
71 MW 12	PB 756 475	47.81	9.331	0.1180	0.511841	-0.9	1.91
Mattawa Klippe: TDM ages < 1.8 Ga							
72 OR 5	PB 685 436	29.37	5.607	0.1154	0.512038	3.4	1.56
73 OR 6	PB 692 433	87.35	16.323	0.1130	0.512004	3.2	1.57
74 OR 17*	PB 709 464	30.42	5.737	0.1140	0.512007	3.1	1.58
75 OR 18*	PB 710 465	60.66	11.919	0.1188	0.511951	1.1	1.75
76 OR 19*	PB 711 467	92.03	16.703	0.1097	0.511913	2.0	1.65
77 OR 20	PB 724 456	57.69	10.883	0.1140	0.512015	3.2	1.57
78 OR 21	PB 733 468	22.84	4.264	0.1128	0.511966	2.5	1.62
79 OR 22	PB 733 474	48.92	10.268	0.1269	0.512018	0.9	1.80
80 OR 25	PB 623 467	32.53	5.731	0.1065	0.511993	4.2	1.49
81 OR 27	PB 625 465	31.05	4.966	0.0967	0.511963	5.4	1.40
82 OR 30	PB 6941 4351	41.87	7.604	0.1098	0.511972	3.2	1.57
83 OR 32	PB 6968 4345	30.20	5.525	0.1106	0.511991	3.4	1.55
84 OR 33	PB 6870 4295	26.70	4.412	0.0999	0.511946	4.5	1.47
85 MW 3	PB 768 454	37.55	6.938	0.1117	0.511951	2.4	1.63
86 MW 4	PB 753 445	35.13	6.737	0.1159	0.512021	2.3	1.59

Sample	Grid Reference	Nd ppm	Sm ppm	$^{147}Sm/^{144}Nd$	$^{143}Nd/^{144}Nd$	eNd 1450	T_{DM} (Ga)
Published Data after Dickin and Guo (2001)							
Reworked Archean parautochthon: TDM ages 1.9-2.6 Ga							
87 MT 49	PB 747 365	4.06	0.63	0.0942	0.511134	-7.0	2.45
88 MT 99	PB 709 421	79.30	11.90	0.0908	0.511390	-1.3	2.05
89 MT 100	PB 727 403	24.51	5.19	0.1281	0.511639	-4.6	2.52
90 MT 82	PB 747 396	68.49	12.51	0.1104	0.511510	-3.2	2.27
91 MT 80	PB 745 386	98.12	18.03	0.1111	0.511634	-0.9	2.09
Mattawa Klippe: TDM ages < 1.8 Ga							
92 MT 47	PB 604 422	34.56	6.36	0.1112	0.511901	4.3	1.70
93 MT 48	PB 637 388	98.98	17.43	0.1064	0.511903	5.4	1.62

* Based on average of two dissolutions
Average error on isotope dilutions was 0.06 % (1σ)
Average error on Nd isotope ratios was 0.011/mil (1σ)

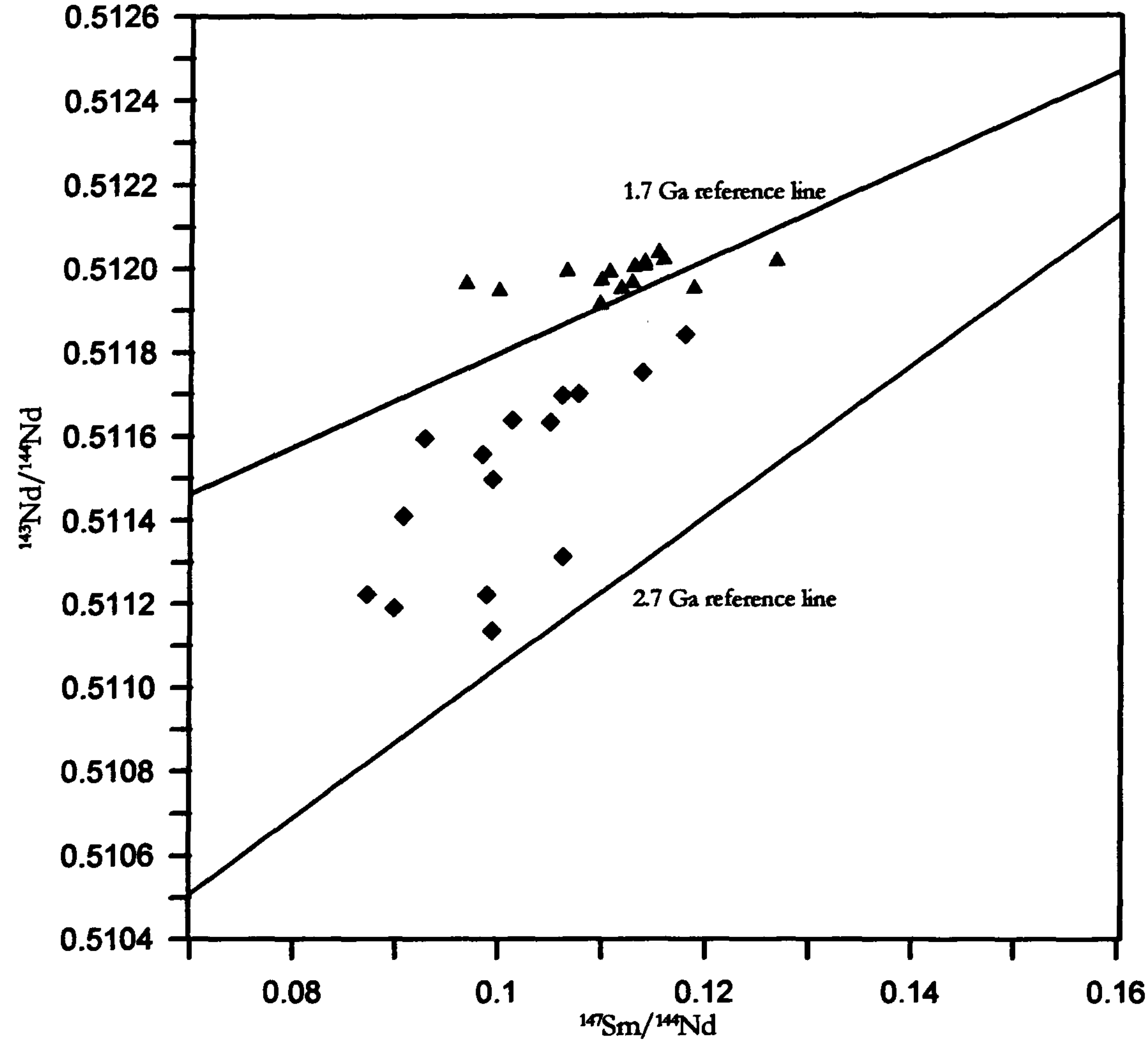

Figure 4.2: Sm-Nd isochron showing geochemical separation of the samples into two fields. Symbols are the same as Figure 4.1.

Figure 4.3 is a plot of epsilon-Nd versus concentration at 1450 Ma. This figure also illustrates the discrimination of the samples into two separate fields. It is seen in figure 4.3 that mid-proterozoic allochthonous units have high epsilon-Nd values (+0.9 to +5.4) and a wide range of Nd concentrations whereas reworked Archean parautochthonous units have lower epsilon-Nd values (-0.9 to –11.3) with an associated wide range of Nd concentrations. There are two reworked Archean samples (samples 65 and 69) that have extremely low epsilon-Nd values and low Nd concentrations, separating them from the main cluster. This deviation is the result of their Nd-model ages, which are 2.46 and 2.56 Ga respectively, indicating that these rocks are too young to be considered as pristine Archean rocks, but have been less reworked than the other "reworked Archean" counterparts.

In Figure 4.3 the distinction between the reworked Archean parautochthon and the mid-Proterozoic allochthon is less obvious. However, the separation of the two crustal units is more clearly illustrated in Figure 4.4. Figure 4.4 is a histogram plot showing the frequency of εNd values calculated at 1.45 Ga. Samples from the northern section of the study area are also included to provide a more comprehensive dataset. Two major peaks are seen in this diagram representing two different crustal terranes. Rocks with epsilon-Nd values from +0 to +6 are attributed to the allochthonous structures within the study area whereas the epsilon-Nd range from –10 to 0 represents the reworked Archean parautochthon. It is seen between these two peaks that there is some overlap as a result of some units being more intensely reworked than others.

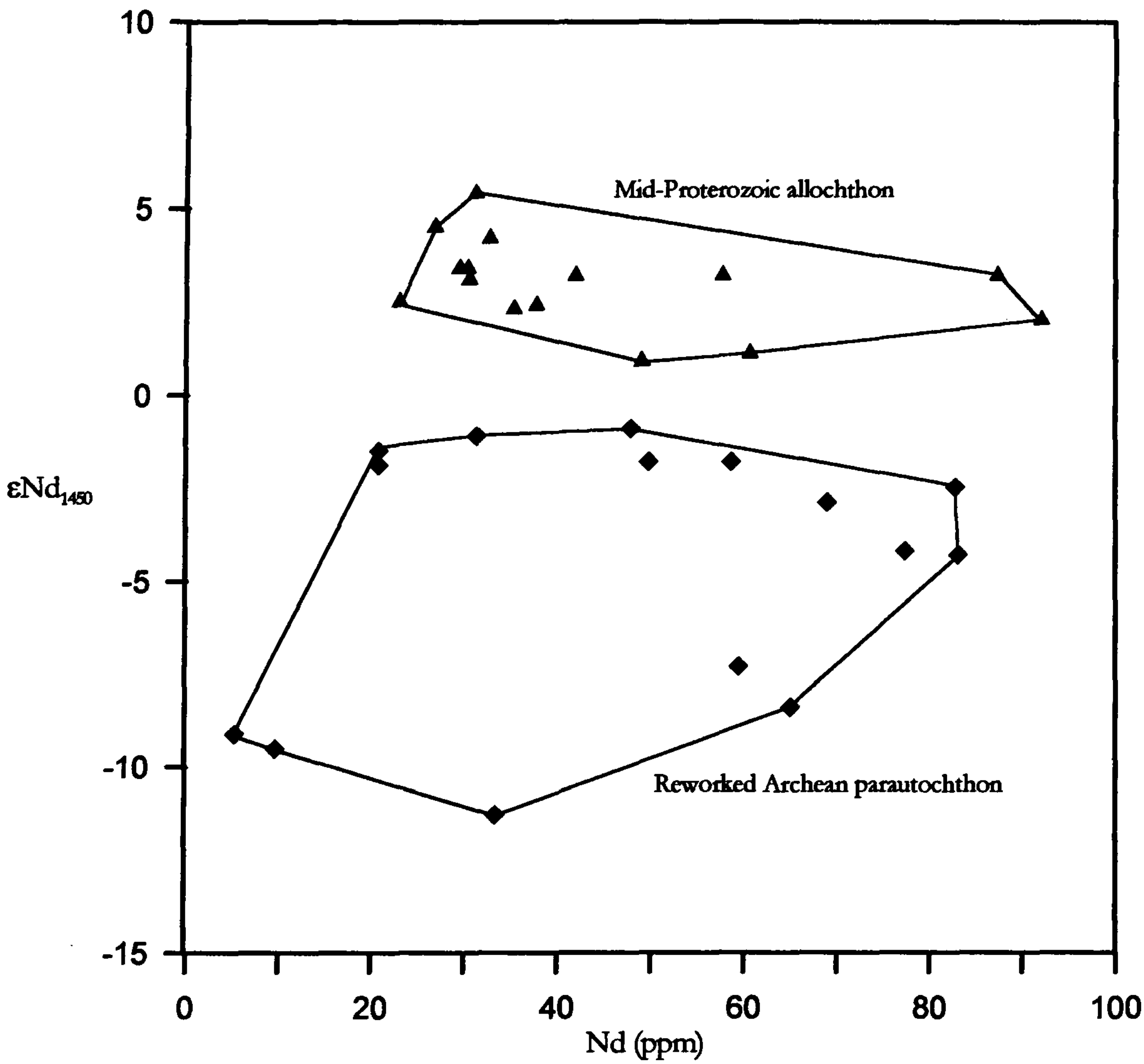

Figure 4.3: Plot of εNd (t) versus concentration. Symbols are the same as Figures 4.1 and 4.2.

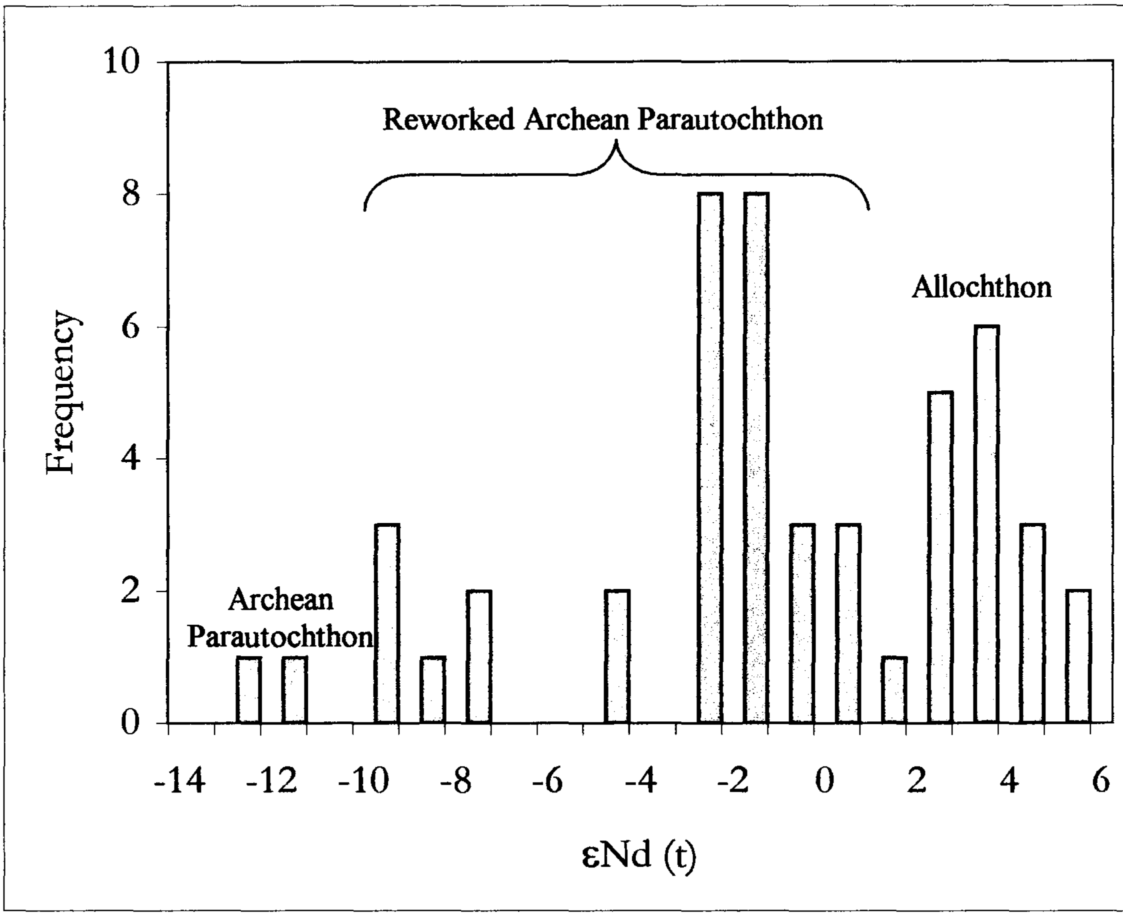

Figure 4.4: Histogram plot showing the frequency of εNd calculated at 1450 Ma.

When the Nd-model ages are examined geographically, a sharp boundary can be drawn between mid-Proterozoic allochthonous crust and reworked Archean parautochthonous crust marking the limits of the Mattawa klippe (Figure 4.1). However, on the Quebec side of the Ottawa river, a nose of reworked Archean crust was found pushing into the klippe (Sample 63). It is possible that this region is more deeply exhumed relative to its eastern and western counterparts allowing the parautochthon to outcrop between two, once cohesive units.

It is concluded that the Mattawa klippe represents an erosional remnant of the once intact APB that was thrust northwestward over the parauthochthon. It is defined here as a remnant location of the APB (Figure 4.1) and is not part of the main allochthon. It is seen that the coronitic metagabbros and eclogites that Ketchum and Davidson (2000) used to define the limits of the allochthon are exclusively contained within the Mattawa klippe (their Figure 5). Therefore, discrimination of metabasic rock types can only be used to determine whether units are allochthonous or autochthonous but should not be used to locate tectonic boundaries without other constraints.

CHAPTER 5

RESULTS: SOUTHERN SECTION

5.1 Geological Context

The northern section of the field area encompasses approximately 7600 km^2 extending from 45° 50′ N, 79° 00′ W in the southwest to 46° 30′ N, 77° 30′ W in the northeast excluding the Mattawa klippe region (Figure 5.1). Detailed Nd-model age mapping has been completed in the northern portion of this region along the Ottawa River (Dickin and Guo, 2001). The Ottawa River has been interpreted as a locus of continental rifting as a result of the Mattawa fault, which forms part of the Ottawa-Bonechere graben. Based on the distribution of Nd-model ages, Dickin and Guo (2001) postulated that the Mattawa fault is a reactivated ancient suture that separated Paleoproterozoic crust (T_{DM} ages: 1.8-1.95 Ga) from reworked Archean crust (T_{DM} ages: 1.9-2.6 Ga). These two units were referred to as the reworked Archean parautochthon and the Paleoproterozoic parautochthon.

It has been mentioned above that the allochthon boundary thrust (ABT) was expected to be located further south than the predictions of Ketchum and Davidson (2000). On figure 5.1 the allochthonous Lac Watson nappe appears in the eastern portion of the region, and based on previous Nd-model age mapping (Dickin and Guo, 2001) it represents the location of the ABT. However, due to the lack of isotopic information in the region, the location of the ABT further southwest is still unknown.

It was the objective of the present study to collect samples south of the Ottawa River to determine the location and attitude of the ABT in this region. Likewise, samples were also collected along the Ottawa River to further constrain the limits of the suture separating the reworked Archean parautochthon from the paleoproterozoic parautochthon.

5.2 Nd-model age mapping

29 new Nd-model ages were calculated on grey orthogneisses using the depleted mantle model of DePaolo (1981) and combined with those of Dickin and Guo (2001) to provide constraints on the suture separating the reworked Archean parautochthon from the Paleoproterozoic parautochthon and also to map the southern limits of the ABT in the region. The geographic distribution of these samples is illustrated in figure 5.1 and the corresponding isotopic data is listed in table 5.1. However, only the Nd isotopic data for the samples analysed in this study are plotted in figures 5.2 and 5.3.

Three Nd-model age ranges were calculated for the region and they form three separate fields in Figure 5.2, which is an isochron plot of $^{143}Nd/^{144}Nd$ versus $^{147}Nd/^{144}Nd$. A 2.7 Ga reference line typical of Archean aged rocks and a 1.7 Ga reference line representing the mid-Proterozoic allochthon (solid triangles) are also included. It is seen that the mid-Proterozoic allochthonous units lie on the 1.7 Ga reference line. Both the reworked Archean parautochthon (solid diamonds) and the Paleoproterozoic

Figure 5.1: Geographical distribution of Nd-model ages illustrating the location of the ABT in the southern region of the study area. Closed diamonds = reworked Archean parautochthon; closed circles = Paleoproterozoic parautochthon; closed triangles = mid-Proterozoic allochthon. Open symbols are the Nd-model age sample locations of Dickin and Guo (2001). Samples 174-177 are after Martin (1992). Axis labels = 10 km UTM grid squares. Geological base map after Lumbers (1976).

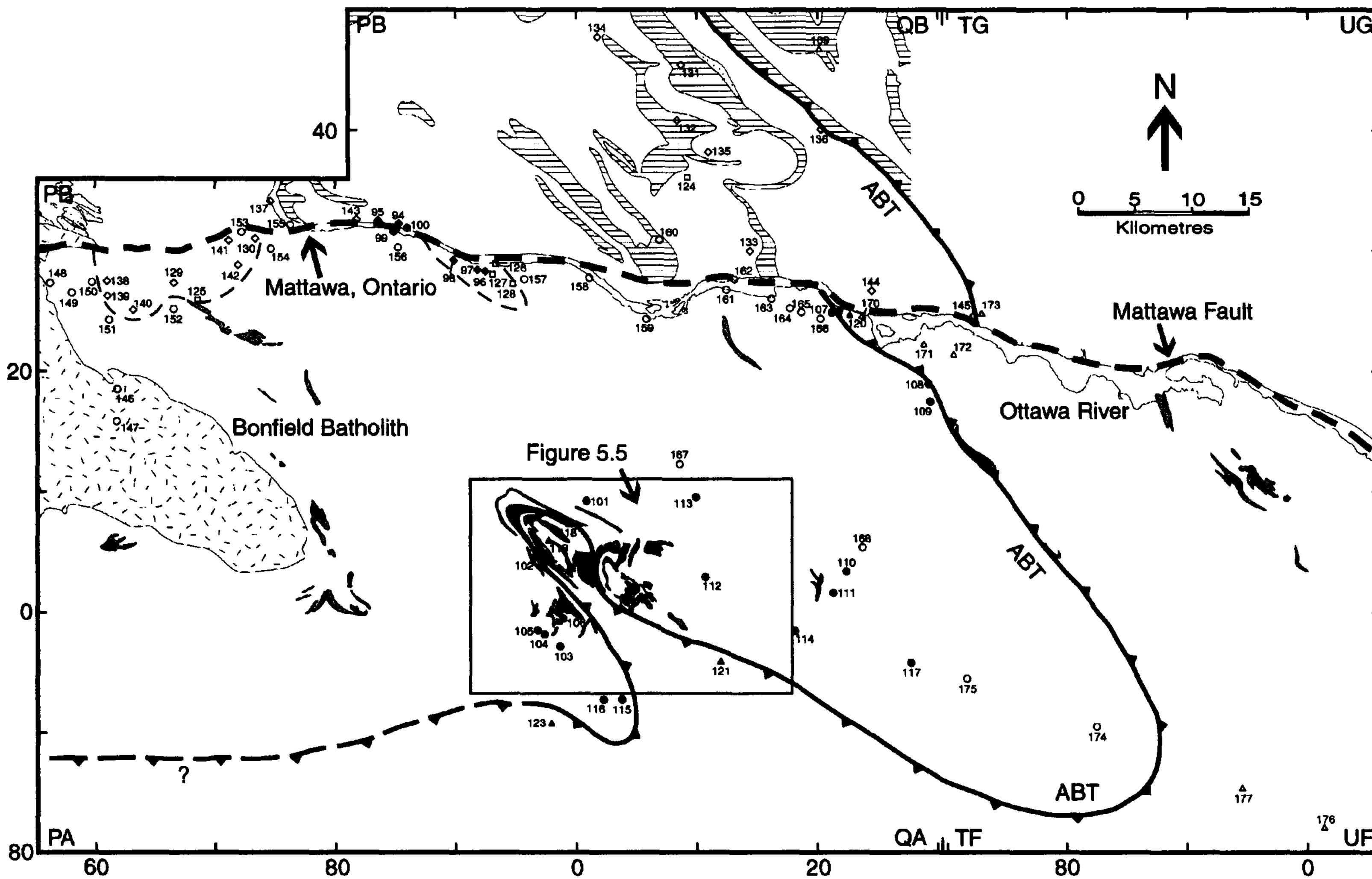
PB
QB
TG
UG
PA
QA
TF
UF
N
0 5 10 15
Kilometres
ABT
Mattawa, Ontario
Mattawa Fault
Ottawa River
Bonfield Batholith
Figure 5.5
40
20
0
80
60
80
0
20
80
0

Table 5.1: Sm-Nd Isotopic Data for the Southern Region

Sample	Grid Reference	Nd ppm	Sm ppm	$^{147}Sm/^{144}Nd$	$^{143}Nd/^{144}Nd$	eNd 1450	T_{DM} (Ga)
New Data							
Reworked Archean parautochthon: TDM 1.9-2.6 Ga							
94OR 12	PB 849 322	95.55	17.312	0.1095	0.511595	-4.2	2.12
95OR 14	PB 832 323	100.32	16.864	0.1016	0.511586	-2.9	1.98
96OR 34	PB 9215 2835	98.00	17.572	0.1084	0.511483	-6.2	2.26
97OR 35	PB 918 285	54.80	8.564	0.0944	0.511333	-6.5	2.19
98OR 36	PB 899 293	64.81	11.815	0.1102	0.511701	-2.2	1.98
Paleoproterozoic parautochthon: TDM ages: 1.8-1.95 Ga							
99OR 10	PB 845 319	44.4	8.278	0.1127	0.511753	-1.7	1.95
100OR 11	PB 856 321	119.69	18.320	0.0925	0.511536	-2.2	1.89
101AQ 10	QB 0025 093	64.11	11.117	0.1048	0.511672	-1.8	1.92
102AQ 11	PB 972 051	78.17	13.393	0.1036	0.511694	-1.1	1.87
103AQ 12	PA 983 974	19.43	2.728	0.0849	0.511515	-1.1	1.81
104AQ 13	PA 970 983	60.08	11.018	0.1109	0.511793	-0.5	1.85
105AQ 14	PA 968 986	32.37	5.454	0.1018	0.511649	-1.7	1.90
106AQ 17	PA 986 995	25.02	4.155	0.1004	0.511623	-1.9	1.91
107AQ 20	QB 2102 2473	54.53	9.585	0.1062	0.511694	-1.6	1.91
108AQ 23	QB 289 191	49.98	9.370	0.1133	0.511846	0.0	1.82
109AQ 24	QB 291 174	39.19	6.506	0.1003	0.511650	-1.4	1.87
110AQ 25	QB 220 035	53.27	8.704	0.0988	0.511652	-1.1	1.84
111AQ 26	QB 2085 016	63.89	13.067	0.1236	0.511960	0.3	1.83
112AQ 27	QB 102 032	80.83	14.640	0.1095	0.511801	-0.1	1.81
113AQ 28	QB 099 099	23.55	3.766	0.0967	0.511614	-1.4	1.86
114AQ 29	QA 181 985	77.94	14.472	0.1122	0.511820	-0.3	1.83
115AQ 31	QA 037 929	29.87	7.972	0.1613	0.512296	-0.1	2.18
116AQ 32	QA 023 928	26.22	4.598	0.1060	0.511710	-1.3	1.89
117AQ 34	QA 276 937	72.66	13.780	0.1146	0.511851	-0.1	1.83
Mid-Proterozoic allochthon: TDM ages <1.8 Ga							
118AQ 1	PB 991 075	29.96	6.859	0.1384	0.512277	3.8	1.55
119AQ 3	PB 9765 0595	45.54	7.716	0.1024	0.511845	2.0	1.64
120AQ 21	QB 2213 2483	37.90	7.482	0.1193	0.511937	0.7	1.78
121AQ 30	QA 116 960	20.54	3.017	0.0888	0.511582	-0.5	1.78
123AQ 33	PA 976 909	120.28	23.152	0.1164	0.511933	1.2	1.73
Published Data after Dickin and Guo (2001)							
Archean parautochthon: TDM ages 2.6-2.9 Ga							
124TA 24	QB 090 361	15.02	2.53	0.1017	0.511136	-8.6	2.61
125MT 45	PB 681 259	29.08	4.70	0.0976	0.510967	-11.1	2.75
126MT 67	PB 933 295	3.89	1.03	0.1140	0.511250	-9.1	2.76
127MT 4	PB 928 281	25.96	4.17	0.0971	0.510978	-10.7	2.72

Sample	Grid Reference	Nd ppm	Sm ppm	$^{147}Sm/^{144}Nd$	$^{143}Nd/^{144}Nd$	eNd 1450	T_{DM} (Ga)
128MT 72	PB 941 276	28.60	5.52	0.1167	0.511307	-8.6	2.75
Reworked Archean parautochthon: TDM 1.9-2.6 Ga							
129MT 1	PB 663 277	7.28	1.27	0.1055	0.511272	-6.8	2.51
130MT 85	PB 730 312	4.21	0.61	0.0875	0.511145	-5.4	2.30
131DR 1	QB 085 475	19.10	2.64	0.0837	0.511001	-7.3	2.40
132TA 27	QB 080 410	16.43	2.69	0.0991	0.511252	-5.8	2.39
133H 176	QB 140 300	14.55	1.75	0.0725	0.510875	-7.4	2.35
134DR 8	QB 013 479	40.95	8.06	0.1189	0.511796	0.5	2.01
135TA 29	QB 105 395	53.55	8.29	0.0936	0.511233	-5.0	2.30
136DR 24	QB 203 404	30.04	6.12	0.1229	0.511521	-5.7	2.57
137MT 56	PB 743 342	117.12	20.76	0.1071	0.511604	-0.7	2.06
138MT 89	PB 604 277	49.57	10.44	0.1273	0.511620	-4.8	2.53
139MT 52	PB 605 263	198.96	31.50	0.0957	0.511322	-3.7	2.23
140MT 110	PB 627 274	82.44	17.48	0.1282	0.511851	-0.4	2.13
141MT 97	PB 710 313	69.30	12.42	0.1083	0.511586	-1.3	2.11
142MT 40	PB 716 290	25.29	3.37	0.0806	0.511089	-4.9	2.24
143MT 93	PB 813 323	89.66	15.81	0.1066	0.511602	-0.6	2.05
144MT 96	QB 241 268	17.14	2.97	0.1043	0.511366	-4.7	2.35
145MT 102	TG 719 248	66.03	12.03	0.1102	0.511678	0.1	2.01
Paleoproterozoic parautochthon: TDM ages: 1.8-1.95 Ga							
146BO 5	PB 479 258	20.66	4.34	0.1270	0.511935	1.5	1.95
147BO 1	PB 492 226	27.80	5.68	0.1235	0.511899	1.5	1.93
148BO 2	PB 522 195	100.60	20.22	0.1215	0.511861	1.2	1.95
149MT 37	PB 615 187	38.05	6.36	0.1010	0.511641	1.4	1.90
150TA 32	PB 613 160	42.52	8.73	0.1241	0.511908	1.6	1.93
151MT 90	PB 558 276	63.64	9.49	0.0901	0.511486	0.8	1.92
152MT 88	PB 578 267	28.32	4.21	0.0899	0.511529	1.6	1.86
153MT 87	PB 594 274	37.29	6.00	0.0973	0.511632	2.0	1.83
154MT 42	PB 606 244	95.87	12.96	0.0817	0.511456	2.0	1.83
155TA 37	PB 663 252	47.96	8.79	0.1108	0.511735	1.1	1.94
156MT 83	PB 719 317	68.35	12.24	0.1083	0.511717	1.3	1.91
157MT 2	PB 740 303	30.89	5.28	0.1033	0.511679	1.6	1.88
158MT 55	PB 761 321	41.91	6.61	0.0953	0.511599	1.8	1.86
159MT 3	PB 849 305	70.79	11.89	0.1015	0.511619	0.9	1.93
160MT 71	PB 955 276	65.18	11.61	0.1075	0.511692	1.0	1.94
161MT 68	QB 009 285	55.68	9.57	0.1039	0.511649	0.9	1.93
162MT 5	QB 055 257	37.84	7.01	0.1120	0.511439	0.6	1.92
163TA 21	QB 067 308	104.29	14.95	0.0867	0.511439	0.6	1.92
164MT 65	QB 118 278	68.72	10.96	0.0964	0.511591	1.4	1.88
165MT 62	QB 125 284	43.52	6.85	0.0954	0.511596	1.8	1.86
166MT 7	QB 157 262	30.32	4.55	0.0906	0.511526	1.4	1.88
167H 171	QB 174 252	70.94	9.69	0.0826	0.511417	1.0	1.89

Sample	Grid Reference	Nd ppm	Sm ppm	$^{147}Sm/^{144}Nd$	$^{143}Nd/^{144}Nd$	eNd 1450	T_{DM} (Ga)
168TA 4	QB 179 249	48.77	8.26	0.1024	0.511684	1.9	1.86
169MT 60	QB 201 245	118.14	20.87	0.1068	0.511703	1.2	1.91
170AQ 7	QB 083 125	28.08	4.44	0.0955	0.511591	1.6	1.87
171AU 4	QB 230 053	34.47	5.49	0.0955	0.511612	2.0	1.84
Lac Watson nappe: TDM ages <1.8 Ga							
172DR 27	QB 201 468	26.88	4.63	0.1040	0.511896	5.7	1.59
173TA 5	QB 235 250	68.91	13.82	0.1213	0.511983	3.7	1.75
174MT 8	QB 283 221	61.33	11.11	0.1095	0.511863	3.9	1.72
175MT 9	TG 700 212	42.31	8.69	0.1242	0.512086	5.0	1.63
176MT 103	TG 719 248	37.67	7.10	0.1140	0.512002	5.6	1.59
Unpublished Data after Martin (1992)							
Paleoproterozoic parautochthon: TDM ages: 1.8-1.95 Ga							
174AL 6	TF 821 903	18.65	4.150	0.1345	0.512097	NA	1.82
175AL 9	TF 715 945	18.32	2.847	0.0939	0.511630	NA	1.8
Mid-Proterozoic allochthon: TDM ages <1.8 Ga							
176AL 4	UF 015 825	53.09	8.477	0.0965	0.512845	NA	1.56
177AL 5	TF 944 854	51.07	10.705	0.1266	0.512114	NA	1.62

Average error on isotope dilutions was 0.05 % (1σ)
Average error on Nd isotope ratios was 0.011/mil (1σ)

parautochthon units (solid circles) lie between the envelope of the 1.7 and 2.7 Ga reference lines. The distinction between these units is less obvious, however, it is seen that the reworked Archean parautochthonous units are distributed closer to the 2.7 Ga reference line.

Figure 5.3 is a plot of epsilon-Nd versus Nd concentration where the discrimination of the samples into three fields is also seen. Mid-proterozoic allochthonous model ages have high epsilon-Nd values (-0.1 to +3.8) whereas Nd-model ages representative of the reworked Archean parautochthon have relatively low values (-2.2 to –6.5). There is also an intermediate range of values attributed to the Paleoproterozoic parautochthon with a Nd-model age range from 1.8-1.95 Ga. All three fields exhibit a large range of Nd concentrations.

In figure 5.3 the distinction between the different crustal terranes is not very obvious. However, when a histogram of εNd at 1450 Ma is plotted, the three crustal units become clear. In figure 5.4 there is a large peak between epsilon-Nd values –3 and 0. This range represents the Paleoproterozoic parautochthon with the allochthon units found immediately right of these two peaks and the reworked Archean parautochthon immediately to the left. It is expected that this peak represents the Paleoproterozoic parautochthon since the majority of the data fall within this range for this sub-area.

When the geographical distribution of the samples is illustrated (Figure 5.1), the three fields identified by geochemical discrimination also have a unique distribution. It is seen that the majority of the reworked Archean parautochthonous samples are found

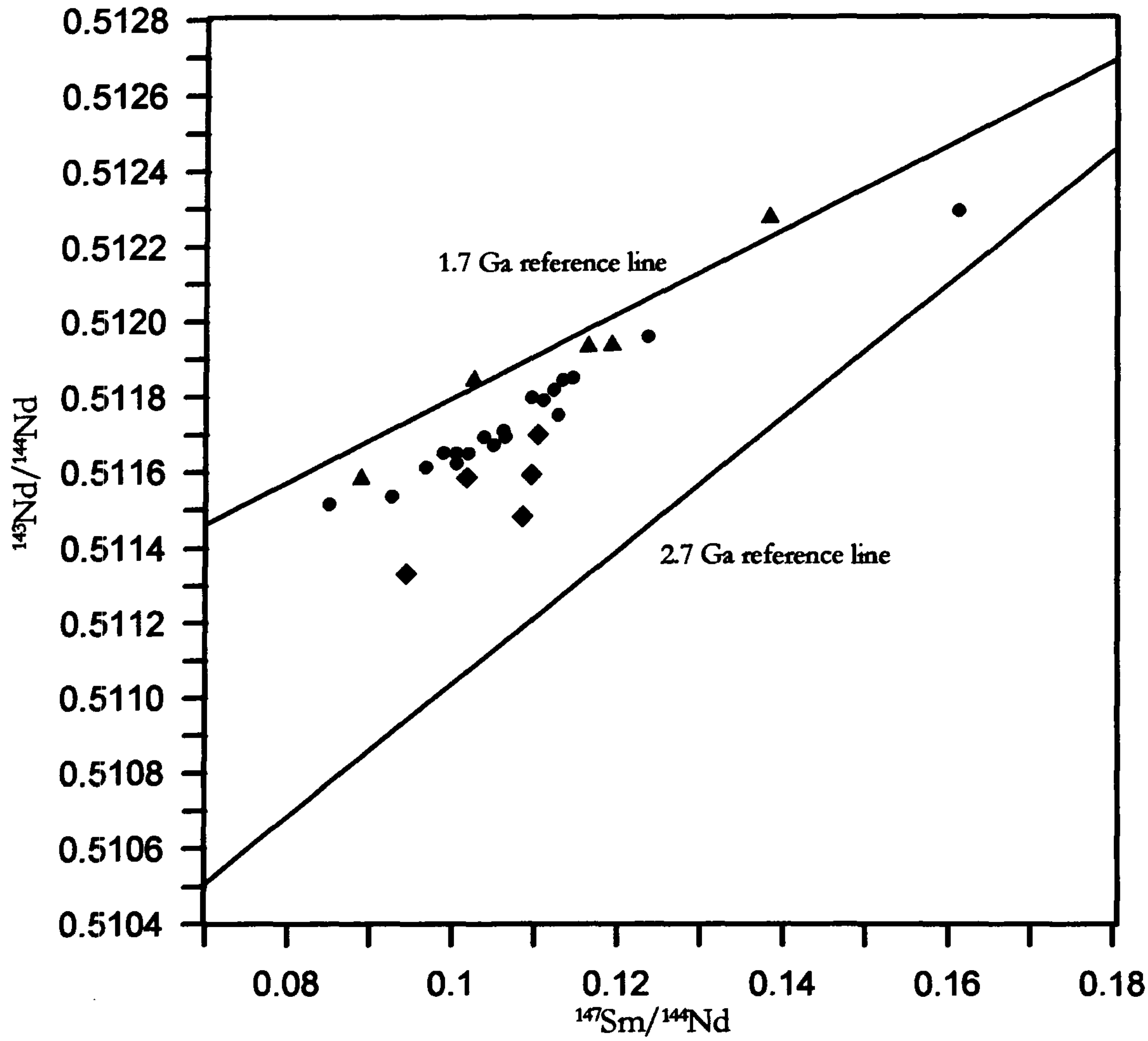

Figure 5.2: Sm-Nd isochron showing geochemical separation of the samples into three fields. Symbols are the same as Figure 5.1.

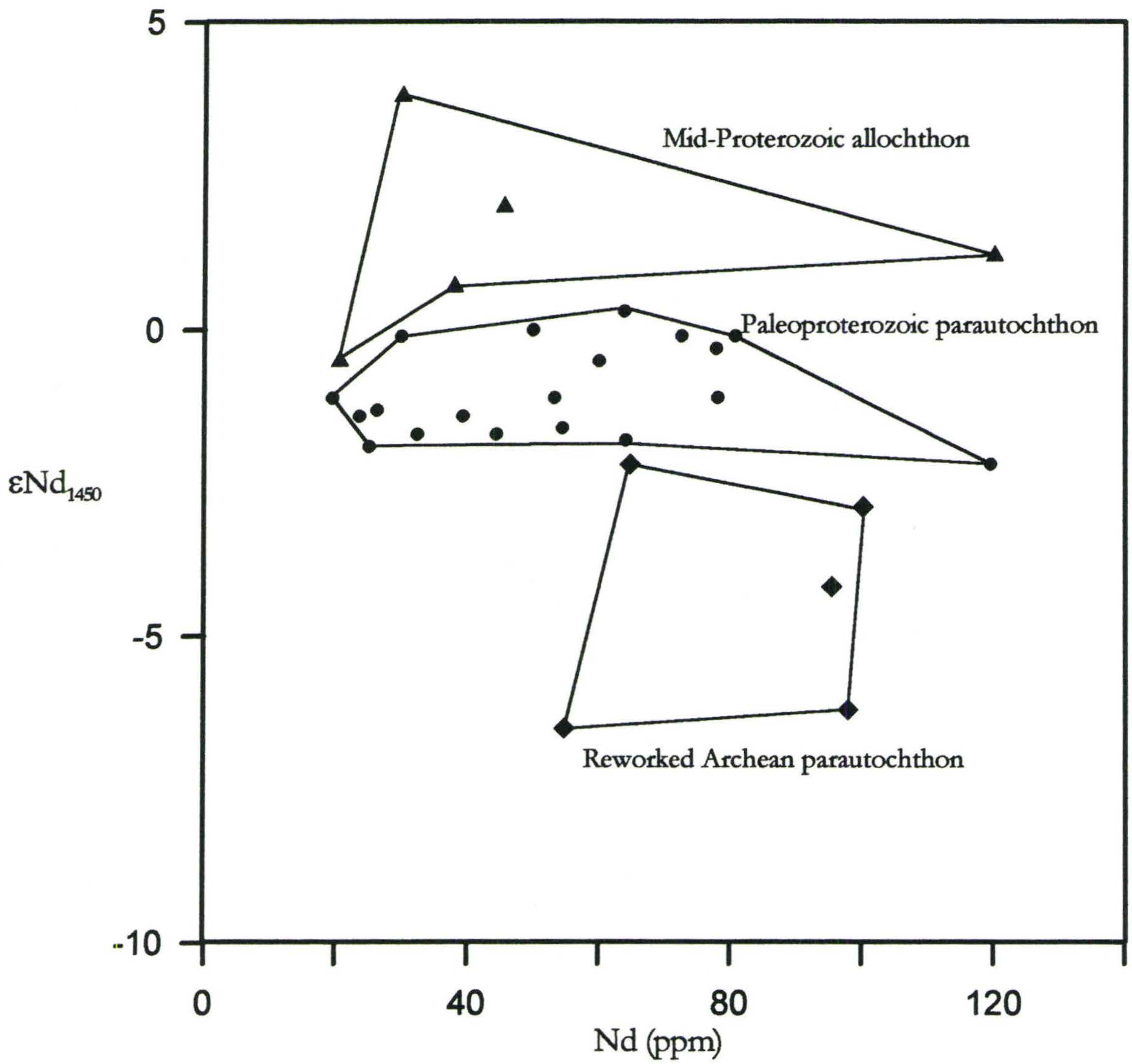

Figure 5.3: Plot of εNd (t) versus concentration. Symbols are the same as Figures 5.1 and 5.2.

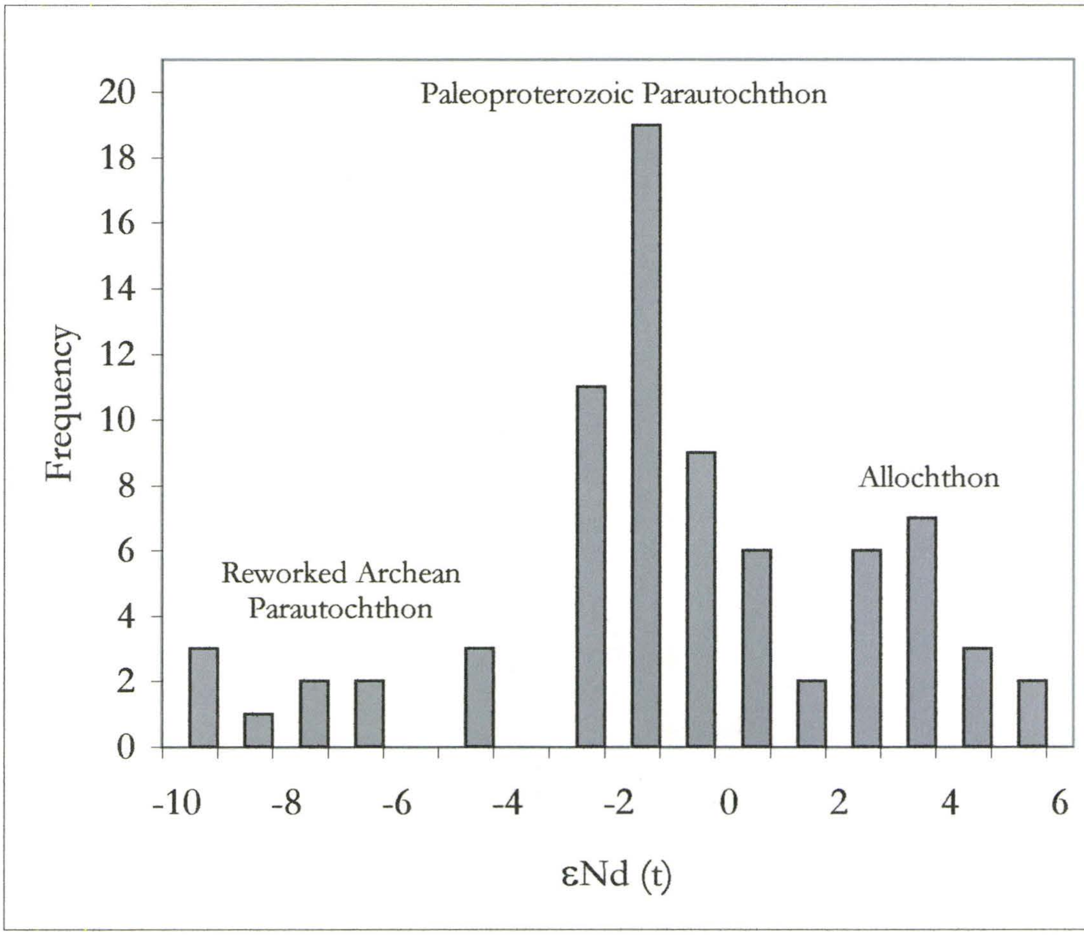

Figure 5.4: Histogram plot showing the frequency of εNd at 1450 Ma including the data from the Mattawa klippe area.

north of the Ottawa River and the majority of the paleoproterozoic parautochthonous samples are located to the south. There is also an occurrence of reworked Archean rocks on the southern side of the Ottawa river indicating that the suture also outcrops to the south of the Mattawa fault (thin dashed line in Figure 5.1). The Mattawa fault is attributed to reactivation of the suture separating these two crustal units (Dickin and Guo, 2001). However, the fault is a brittle fracture and therefore does not follow the exact trace of the suture, which resulted from ductile deformation during the Grenville orogeny and hence the appearance of reworked Archean and Paleoproterozoic aged rocks on the opposing sides of the fault.

Not only does the Mattawa fault offset reworked Archean and Paleoproterozoic rocks, but it also offsets the ABT. When the ABT reaches the fault after travelling southwards along the perimeter of the Lac Watson nappe, it becomes offset right laterally to the south side of the fault. This indicates that the Mattawa fault is a post-Grenvillian fault offsetting units that were emplaced during the Grenville collisional orogeny.

Rocks collected from the Lac Watson nappe are calculated to be allochthonous (T_{DM} ages <1.8 Ga). Therefore, the Lac Watson shear zone is the present day location of the ABT that separates the mid-Proterozoic allochthon from the reworked Archean parautochthon to the north and the Paleoproterozoic parautochthon to the south (Figure 5.1). Further southwest of the Lac Watson nappe, it was found that allochthonous units begin to outcrop again in the northern regions of Algonquin Park, Ontario. This was identified as a probable location of the ABT due to the distribution of mid-Proterozoic allochthonous Nd-model ages in the south versus consistent Paleoproterozoic parautochthonous ages to the north. Here the ABT was mapped to traverse westward towards the Bonfield batholith. However, no samples were collected south of the Bonfield Batholith and the location of the ABT in this region is unknown (dashed ABT line in Figure 5.1).

It is seen in Figure 5.1 that the ABT forms a nosed-shaped nappe in the centre of the field area. Although this resembles the shape of a klippe, based on regional foliations in the region (Lumbers, 1976), it is argued that this actually a narrow nose of the main ABT. Figure 5.5 is a blow-up of this region showing the regional foliations in the area. Only the foliations are illustrated in Figure 5.5 A whereas the foliations are overlain on the geology in Figure 5.5 B. It is seen in Figure 5.5 B that the attitude of the ABT in this region is consistent with the regional foliations indicating that this nose is a narrow portion of the main ABT and not a separate klippe.

Ketchum and Davidson (2000) believed that the ABT followed the Lac Watson nappe northwards and then traversed westward in the north. However, based on Nd-model ages, the opposite is in fact true. The ABT follows the Lac Watson nappe southwards and then traverses westward south of the Bonfield batholith.

Figure 5.5: Regional foliations mapped by Lumbers (1976). Geological base map is also after Lumbers (1976).

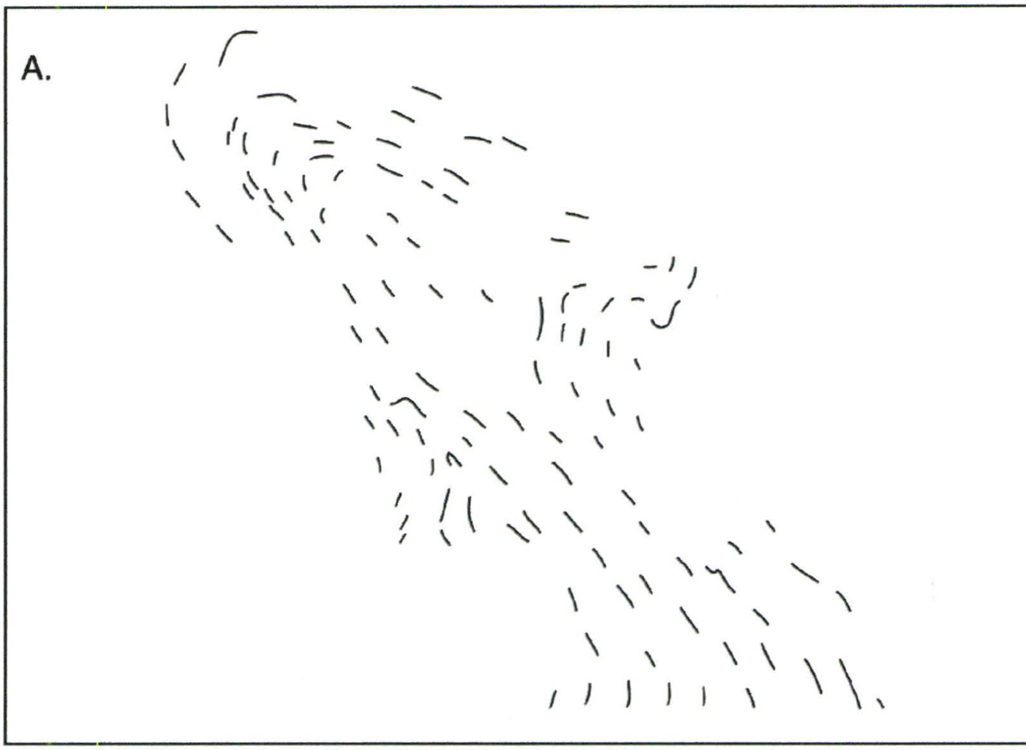
A.


B.

CHAPTER 6

RESULTS: AEROMAGNETIC DATA

6.1 Processing of Aeromagnetic Data

Aeromagnetic data was extracted from a province wide database compiled by the OGS (1993) between 1984 and 1987. Individual aeromagnetic surveys were flown roughly north-south with a mean terrain clearance of 300 m and a flight line spacing of approximately 1000 m over Ontario with some overlap over part of Quebec. The data was imported into Oasis Montaj and then the x, y data was converted to UTM zone 17 coordinates and projected to the NAD 27 datum. The data were then gridded using the minimum curvature algorithm of Briggs (1974). Following this, the data were micro-levelled employing the method of Minty (1991) to remove remaining flight line noise. A regional-residual separation of the data was completed by subtracting an upward continued grid of 500 m from the raw data. The residual data provided the basis for interpretation since this grid represents the high frequency, near surface signal. Finally, the data was reduced to the pole and exported into ERmapper for interpretation.

In ERmapper, the processed magnetic data was colour-draped over a magnetic intensity layer to enhance the visible structures within the area. Many different sunshading angles were used to enhance directional features and also to trace the limits of circular bodies. The final result of these processing steps is seen in Figure 6.1.

Figure 6.1: Location of the final processed aeromagnetic data relative to isotopic data. Image is colour-draped over a magnetic intensity layer in ERmapper with a grid cell spacing of 250 m. Data is projected to the NAD 27 datum, UTM zone 17. Axis labels = 25 km.

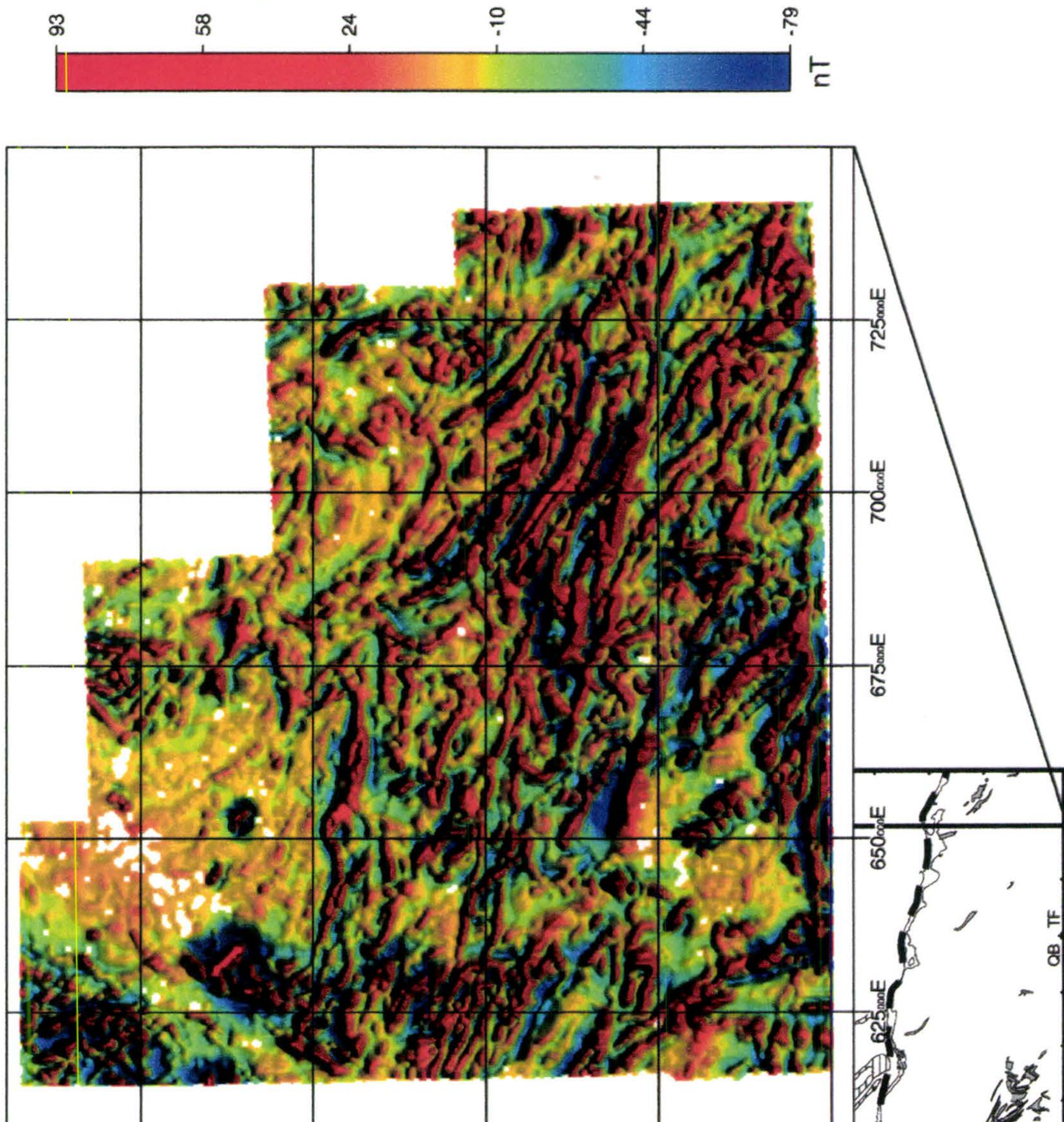
93
58
24
-10
-44
-79
nT
5200000N
5175000N
5150000N
5125000N
5100000N
625000E
650000E
675000E
700000E
725000E
PC
PB
PA
QB
TF

6.2 Interpretation of the Aeromagnetic Data

The residual, reduced-to-the-pole magnetic field map provides the basis of the interpretation of the region. In this manner, all of the high frequency, near surface signal is extrapolated. At a first glance, two different magnetic fabrics are easily distinguished (Figure 6.1). One in which the magnetic signal is characterized by a low lateral magnetic gradient (quiet zone) and another that is characterized by a high lateral magnetic gradient (noisy zone) with variable adjacent magnetic anomalies.

The quiet zone is accentuated in three predominant regions (Figure 6.2) and is interpreted here to represent two different lithological units. In the northern portion of the study area a sharp contact is seen. The geometry of this boundary closely follows the southeast side of the quartzite unit mapped by Rive (1973 a, b) and is interpreted here as the boundary between the Tomiko domain (a meta-quartzite unit overlying the Archean parautochthon (Easton, 1992)) and the underlying Archean parautochthonous gneiss. To the east and the south of this contact, the quiet zone outcrops again. When the geological map for the region is overlain on the aeromagnetic map (Figure 6.3), it becomes evident that these two regions also represent the meta-quartzite of the Tomiko domain. All of the limits of the Tomiko domain are bounded by the noisy zone, identifying the northwestern limit where the reworked Archean parautochthon was thrust over the pristine Archean parautochthon. Hence a boundary between these two crustal units similar to the Nd-model age boundary (see above) can be drawn (Figure 6.4).

It is important to note that at the limits of the Tomiko domain, the meta-quartzite is characterized by high magnetic anomalies indicating the presence of an iron-rich facies.

Figure 6.2: Locations of the quiet zone outlining the Bonfield batholith and the Tomiko domain. Grid cell spacing is 250 m and the data is projected to the NAD 27 datum, UTM zone 17. Axis labels = 25 km.

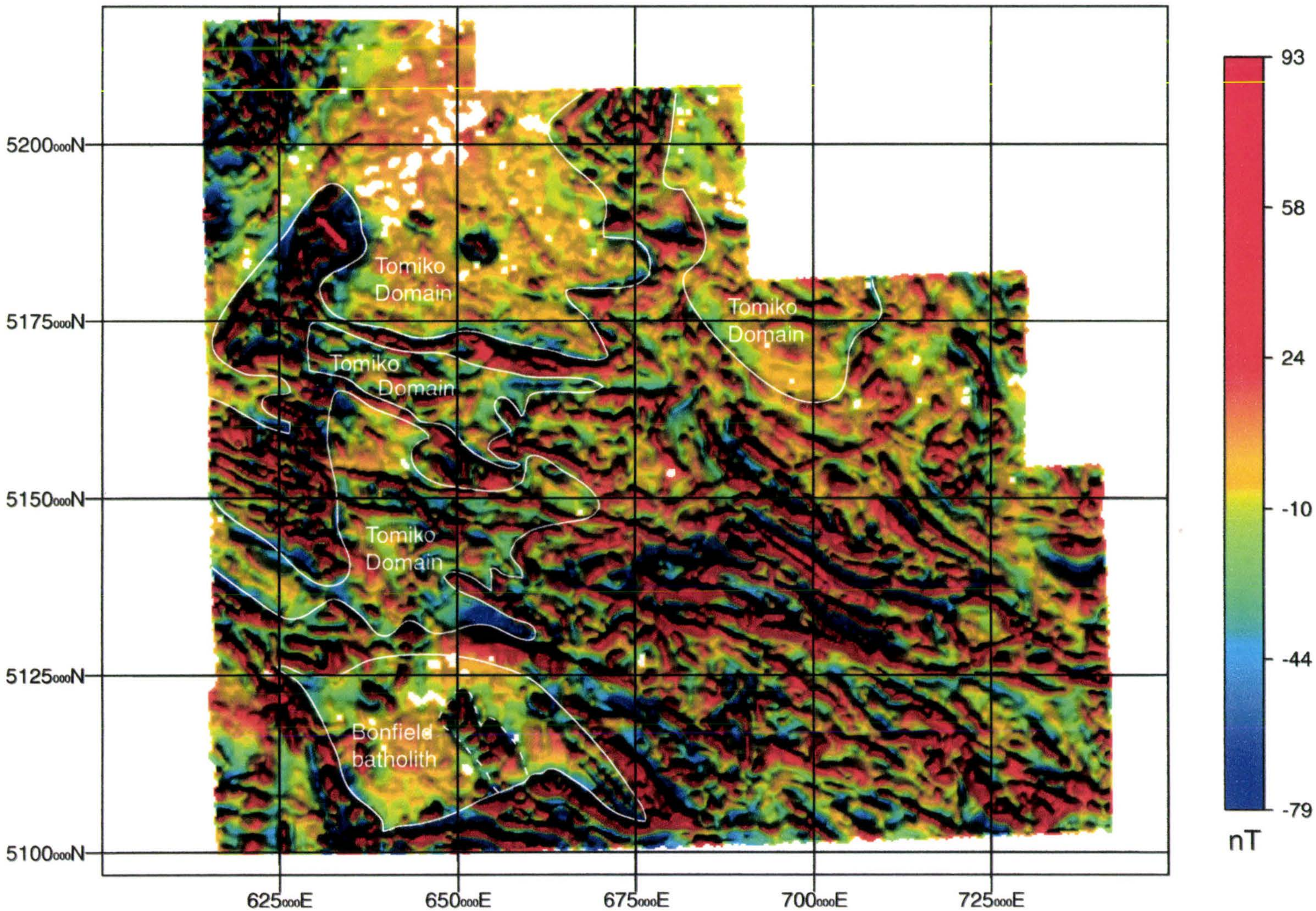

Tomiko Domain
Tomiko Domain
Tomiko Domain
Tomiko Domain
Bonfield batholith
5200000N
5175000N
5150000N
5125000N
5100000N
625000E
650000E
675000E
700000E
725000E
93
58
24
-10
-44
-79
nT

Figure 6.3: Geological map from previous chapters overlain on the aeromagnetic map. Grid cell spacing is 250 m and the data is projected to the NAD 27 datum, UTM zone 17. Axis labels = 25 km.

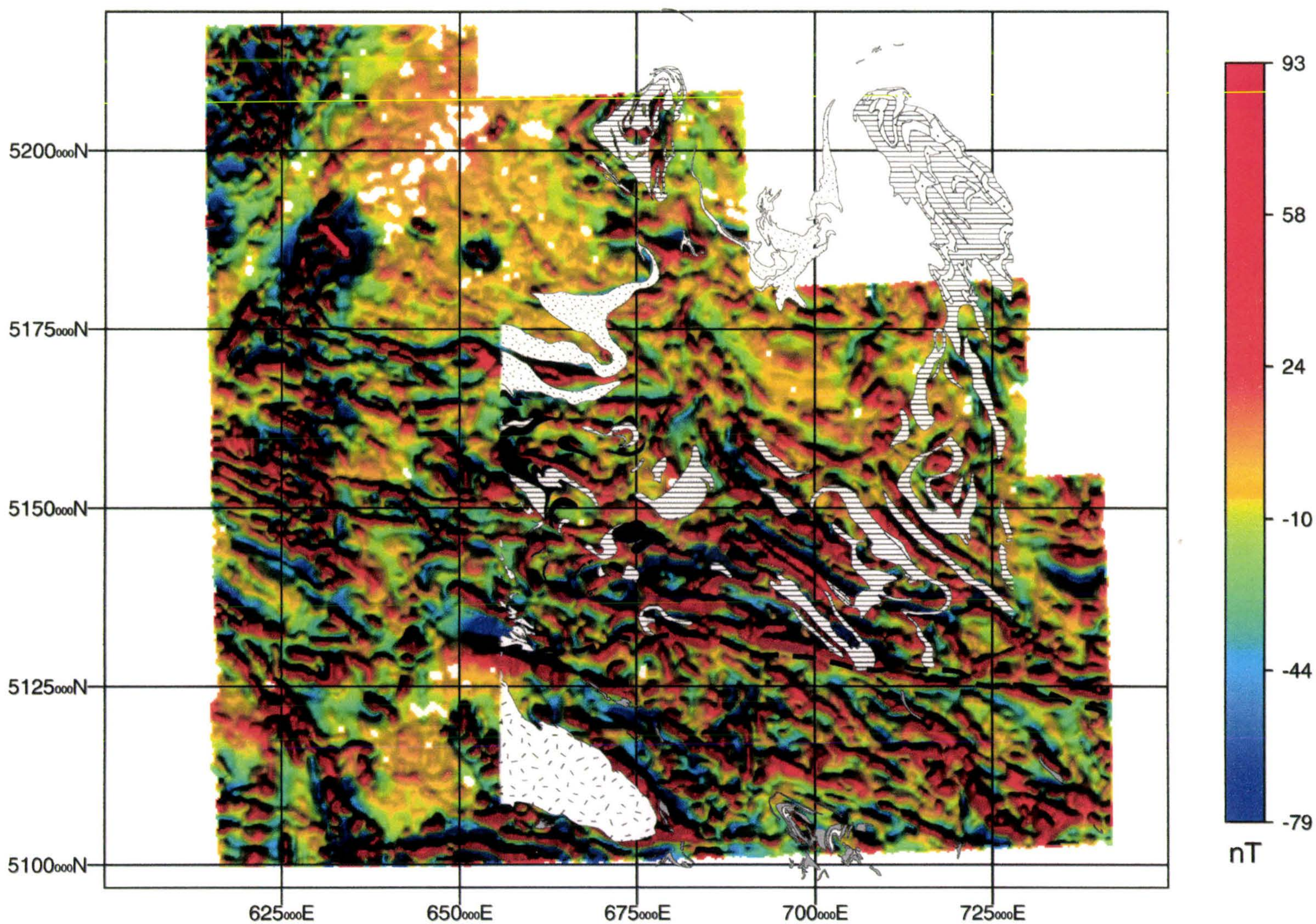

5200000N
5175000N
5150000N
5125000N
5100000N
625000E
650000E
675000E
700000E
725000E
93
58
24
-10
-44
-79
nT

Figure 6.4: Location of the boundary separating the pristine Archean parautochthon from the reworked Archean parautochthon (thick black line). Grid cell spacing is 250 m and the data is projected to the NAD 27 datum, UTM zone 17. Axis labels = 25 km.

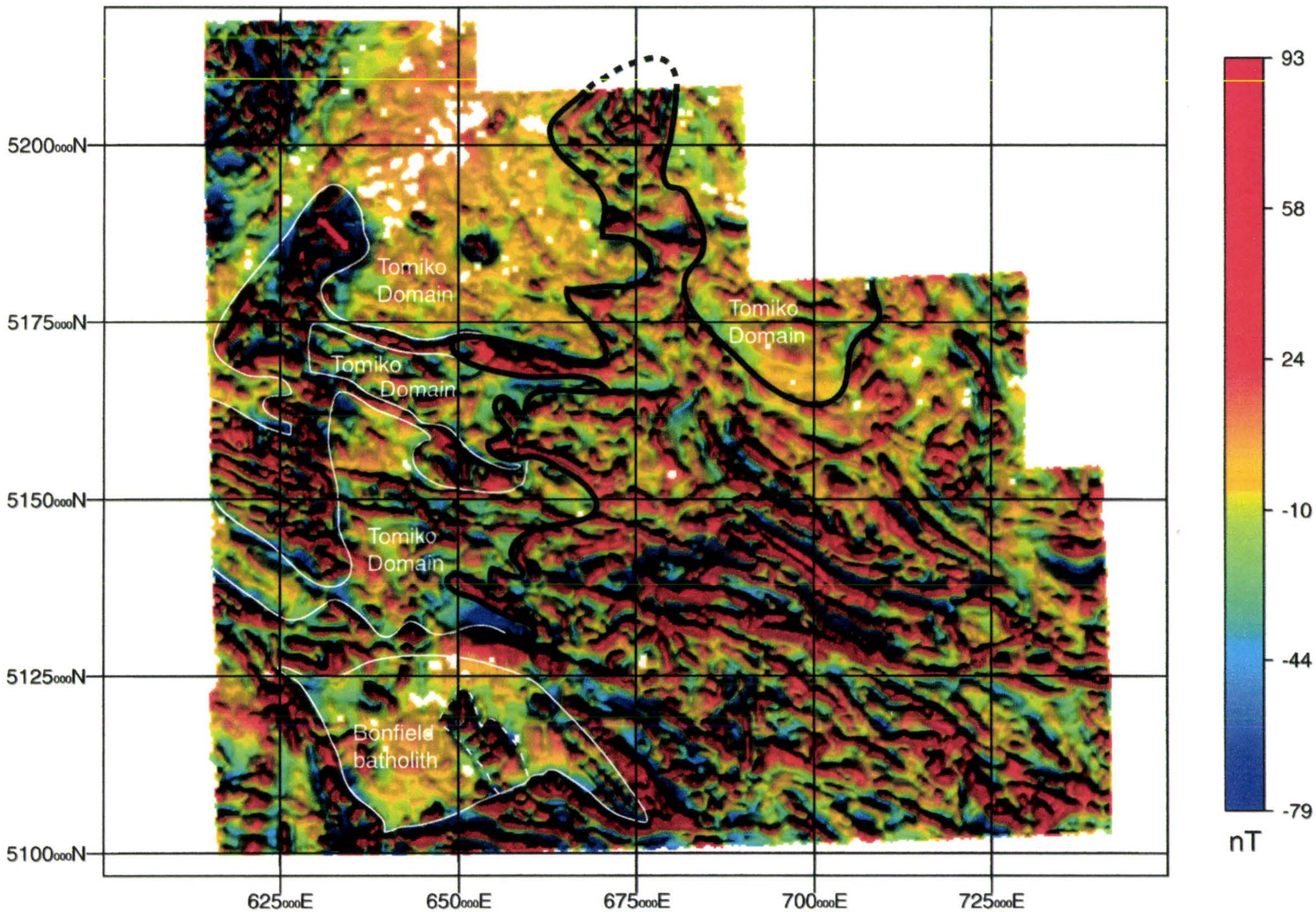

5200000N
5175000N
5150000N
5125000N
5100000N
625000E
650000E
675000E
700000E
725000E
Tomiko Domain
Tomiko Domain
Tomiko Domain
Tomiko Domain
Bonfield batholith
93
58
24
-10
-44
-79
nT

This may be a natural phenomenon where the sediment was derived from an iron-rich substrate, however, since the majority of the high anomalies occur near geological contacts, the magnetic signatures of these iron-rich zones were probably intensified by secondary crystallisation of iron-rich minerals during orogenesis.

The third location of the quiet zone is seen in the southwest corner of the study area. This boundary is interpreted as the geologically well-constrained Bonfield batholith (Lumbers, 1976). However, it is also seen that there is a pronounced change in magnetic fabric within the Bonfield batholith (outlined in Figures 6.2 and 6.4). The magnetic signature of this isolated region within the batholith is similar to the magnetic signature of the rock units immediately to the east of the batholith. It is likely that at the time of emplacement of the batholith into this crustal unit it never reached the surface. However, following years of erosion, the batholith was later exposed. Since the magnetic signature of this isolated region within the batholith represents the magnetic signature of the crustal units that the batholith was intruded into, this isolated region is interpreted as an erosional window where crustal rock overlying the batholith was not completely exhumed or the batholith is very thin here and the underlying units are dominating the magnetic signal.

Within the noisy zone, many geological structures can be identified by continuous curvilinear magnetic anomalies. Of these, previously mapped allochthonous structures such as the Lac Watson nappe (Indares and Dunning, 1997), the Lac Booth klippe (Kellet et al., 1994), and the Mattawa klippe (Dickin and Guo, 2001) are easily identified by continuous magnetic anomalies outlining the limits of their bodies (Figure 6.5). These structures are the isolated allochthonous remnants of an eroded mid-Proterozoic thrust

Figure 6.5: Location of previously mapped allochthonous units and unmapped folded structures and the location of faults within the region based on the aeromagnetic signal. Grid cell spacing is 250 m and the data is projected to the NAD 27 datum, UTM zone 17. Axis labels = 25 km.

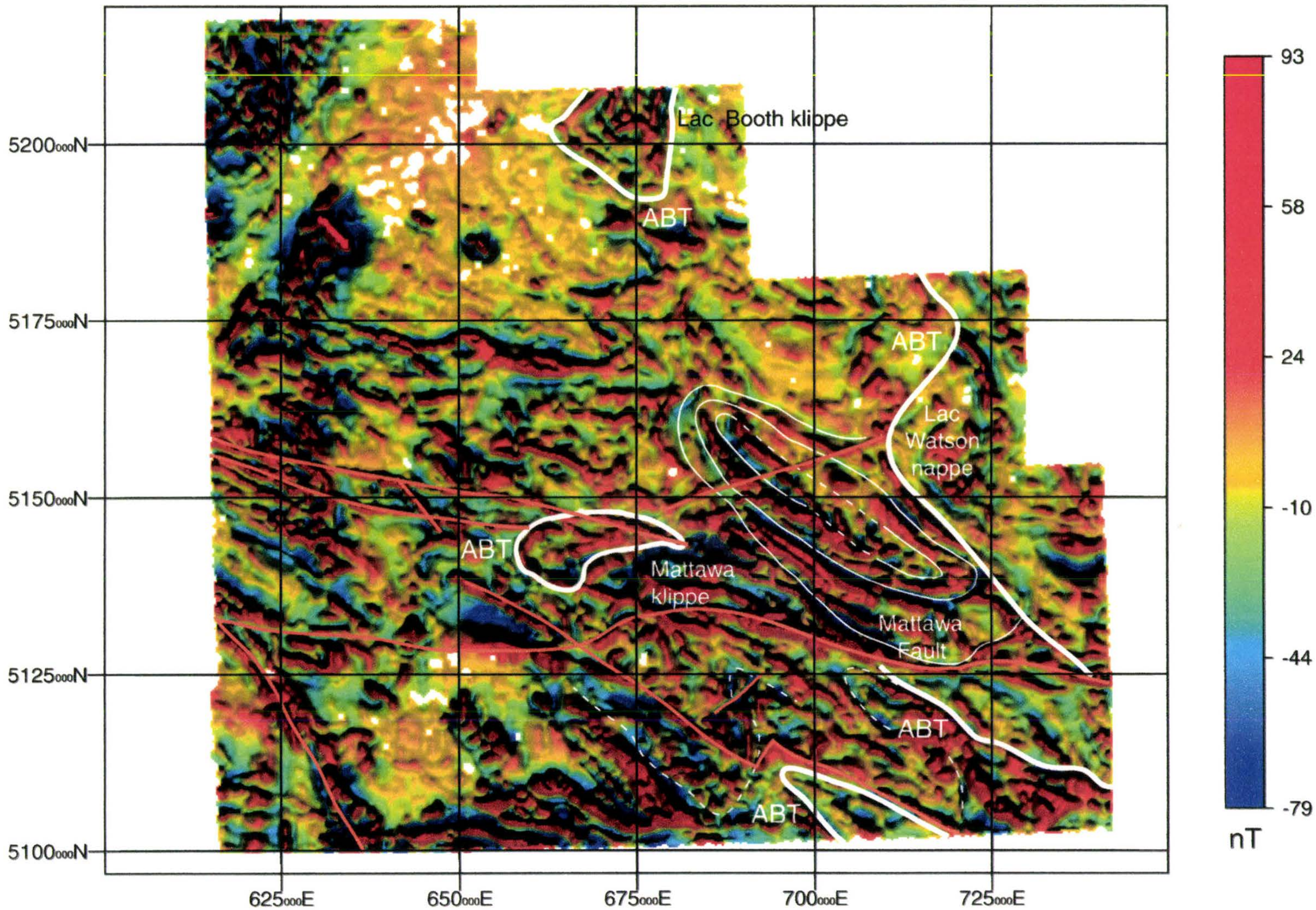
Lac Booth klippe
ABT
ABT
Lac Watson nappe
ABT
Mattawa klippe
Mattawa Fault
ABT
ABT
5200000N
5175000N
5150000N
5125000N
5100000N
625000E
650000E
675000E
700000E
725000E
93
58
24
-10
-44
-79
nT

sheet overlying both pristine and reworked Archean crust (Dickin and Guo, 2001) and represent erosionally isolated equivalents of the allochthon boundary thrust (ABT) (thick white line in Figure 6.5).

Some previously unmapped, less noticeable folded structures are also identified by curvilinear anomalies seen in the magnetic signal (Figure 6.5). In figure 6.5 there is an elliptical folded structure in the northeast portion of the study area east of the Mattawa klippe. It is possible that folding in this region is associated with the northwestward movement of the Lac Watson nappe, causing crustal shortening and thickening as a result of compressive forces. To the south of the study area, many minor folds are identified and are most likely associated with the northwestward movement of the Lac Watson nappe in the east and the emplacement of the Bonfield batholith in the west. However, one structure with the geometry of a fold in the southeast section west of the Lac Watson nappe is marked as the location of the ABT (thick white line in Figure 6.5) based on its magnetic similarities to the Lac Watson nappe and the presence of allochthonous Nd-model ages in the region (see above).

The aeromagnetic data of the study area not only identifies the location of folded structures, but also marks the location of various faults seen in the region (Figure 6.5). The largest fault identified in the region is the Mattawa fault, which is an east-west trending right lateral fault and is marked by the offset of magnetic anomalies of the geological units to the north relative to the magnetic anomalies of the geological units in the south. The Mattawa fault is also emphasized by the lack of correlation between folded structures in the crustal units on opposing sides of the fault as a result of vertical displacement (Figure 6.5). The only structure where displacement is immediately obvious is along the western margin of the Lac Booth klippe. Here a right lateral displacement of more than 20 km can be seen. Since the Lac Watson nappe has been argued to be the location of the ABT, the ABT also exhibits the same lateral offset indicating that the Mattawa fault is a post-Grenvillian structure.

To the north of the Mattawa fault, many splaying faults can be identified based on breaks in the magnetic anomalies (Figure 6.5). These roughly sub-parallel, east-west trending faults are part of the Ottawa-Bonnechere graben system (Kay, 1942).

CHAPTER 7

DISCUSSION AND CONCLUSIONS

7.1 Discussion

In correctly identifying the Shawanaga shear zone as a suitable location for the allochthon boundary thrust (ABT), Ketchum (1994) noticed that the ABT in this region separated two distinct metabasic rock lithologies. He noted that the footwall of the thrust (parautochthon) contained 1.24 Ga metabasic rocks similar to the Sudbury diabase dike swarm whereas the hanging wall (allochthon) exclusively hosted 1.16 Ga coronitic metagabbros. Ketchum and Davidson (2000) argued that the entire ABT could be traced based on the discrimination of these two metabasic rock types into their corresponding first-order belts. Employing this method, Ketchum and Davidson (2000) mapped the ABT within the vicinity of Mattawa, Ontario. However, the distribution of these two types of metabasic rocks is not evenly distributed within the field area (see their Fig. 2). Only two clusters of the 1.16 Ga coronitic metagabbros were mapped; one where these metagabbros are confined within the Lac Booth klippe and another cluster near Mattawa, Ontario. They identified the remaining portion of the ABT by postulating that the limits of the Tomiko Domain, a quartzite cratonic sedimentary sequence overlying the Archean parautochthon (Easton, 1992), represented the southeastern limit of the parautochthon.

More recently Dickin and Guo (2001) argued that this methodology is not suitable for mapping the ABT in the vicinity of Mattawa, Ontario due to the presence of allochthonous klippen that may host 1.16 Ga metagabbros, indicating that the ABT is actually located further south than the location proposed by Ketchum and Davidson (2000). Three allochthonous units have been identified within the study area: the Lac Watson nappe in the east (Indares and Dunning, 1997), the Lac Booth klippe (Kellet et al., 1994) in the north and the Mattawa klippe (Dickin and Guo, 2001) in the west. Both the Lac Booth klippe and the Lac Watson nappe are geochronologically well constrained, however, the Mattawa klippe was only mapped based on the presence of two mid-Proterozoic Nd-model ages and the presence of retrogressed ecologite in the area. Therefore, the extent and geometry of the Mattawa klippe was incomplete.

Based on Nd-model mapping in the present study, it was found that Ketchum and Davidson's (2000) two clusters of 1.16 Ga metagabbros assigned to the allochthonous polycyclic belt (APB) are completely contained within allochthonous klippen. Detailed Nd-model age mapping was employed in the region of the Mattawa klippe. The limits of the klippe were traced between crustal units with a mid-Proterozoic Nd-model age of 1.59 Ga and crust with an average model age of 2.1 Ga. Based on the limits of these two crustal units, the 1.16 Ga coronitic metagabbros identified by Ketchum and Davidson (2000) are all contained within the Mattawa klippe.

In the northern region of the study area, Ketchum and Davidson (2000) also identified a cluster of 1.16 Ga coronitic metagabbros, which they assigned to the Lac Booth klippe indicating that this is an erosional remnant of the APB. The Nd-model ages in the present study confirm that this is an allochthonous klippe, however, it was found that the shear zone at the base of the Lac Booth klippe separates allochthonous crust with an average Nd-model age of 1.5 Ga from reworked Archean crust with an average Nd-model age of 2.0 Ga.

Where metabasic rocks were absent, Ketchum and Davidson (2000) proposed that the ABT could be traced along the limits of the Tomiko domain. Although the limits of this domain mark the limit of a tectonic boundary, it does not represent the limit of the northeastward thrusting of the APB. Along the limits of this boundary, a break in Nd-model ages is observed. Orthogneissic rocks within the Tomiko domain are characterized with Archean Nd-model ages greater than 2.6 Ga whereas orthogneissic units outside of the domain have a reworked Archean Nd-model age range between 1.9-2.6 Ga. Therefore, the limits of the Tomiko domain can be traced to map the boundary between pristine Archean and reworked Archean crust but it does not represent the location of the ABT.

A similar tectonic boundary further south in the study area also marks a break in Nd-model ages along the Mattawa fault. North of the fault it was found that the majority of the samples collected exhibited reworked Archean affinities (1.9-2.6 Ga). Conversely, immediately south of the Mattawa fault orthogneissic samples are characterized by a Paleoproterozoic Nd-model age range (1.8-1.95 Ga). Based on previous Nd-model ages (Dickin and Guo, 2001) and Nd-model ages in this study, it is postulated that this break in Nd model ages represents an ancient suture between the reworked Archean parautochthon and a Paleoproterozoic parautochthon.

The final break in Nd-model ages is found approximately 30 km south of the Mattawa fault. Here the Paleoproterozoic parautochthon is truncated by a mid-Proterozoic allochthonous terrane representing the northeast limit of the APB. Based on the distribution of mid-Proterozoic allocthonous Nd-model ages in this region, the location and attitude of the ABT was mapped. It is interpreted to follow the geometry of the allocthonous Lac Watson nappe southwards to the Mattawa fault. Beyond the Mattawa fault, the nappe is offset causing an offset of the ABT. Finally the ABT continues southwards until the end of the Lac Watson nappe where it then begins to traverse westward within Algonquin park. South of the Bonfield batholith, the location and attitude of the ABT is still uncertain due to the absence of samples in the region. It is provisionally drawn to continue directly westwards south of the batholith but more work is needed in this region to locate the direction of the ABT in this region.

Four distinct Nd-model age ranges were identified in the region of Mattawa, Ontario, which are demarcated by three tectonic boundaries. Likewise, based on the distribution of Nd-model ages, two thrusting events have been identified. The evolution of these thrusting events is shown in Figure 7.1 and explained as follows. Before 1.2 Ga, the four different crustal units formed parallel belts within the Laurentian craton (Figure 7.1 A). When this continent collided with another continental mass to the southeast, northwest directed compression caused the APB to be thrust over the PB (Figure 7.1 B). Compressional forces associated with the northwestward thrusting of the APB caused the cutting down of the thrust zone so that the reworked Archean parautochthon became

Figure 7.1: Evolution of the Grenville Province in the Mattawa, Ontario Region. A. Initial alignment of the Archean, reworked Archean, Paleoproterozoic parautochthons and the mid-Proterozoic allochthon. B. Thrusting of the allochthon and the reworked Archean parautochthon over the Archean parautochthon. C. Appearance of the crustal terranes after exhumation. D. Reactivation of the Mattawa fault.

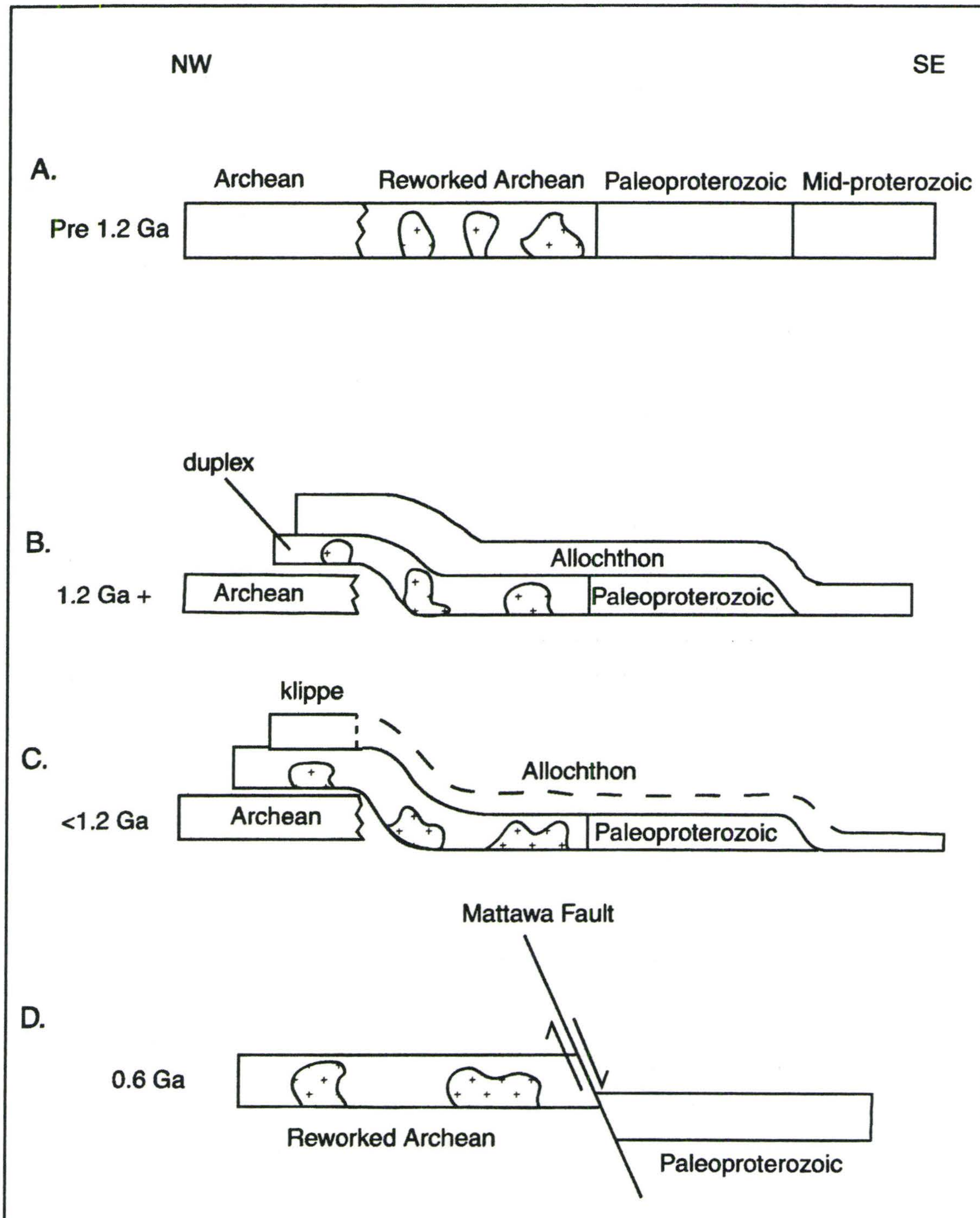
NW
SE
A.
Archean
Reworked Archean
Paleoproterozoic
Mid-proterozoic
Pre 1.2 Ga
duplex
B.
Allochthon
1.2 Ga +
Archean
Paleoproterozoic
klippe
C.
Allochthon
<1.2 Ga
Archean
Paleoproterozoic
Mattawa Fault
D.
0.6 Ga
Reworked Archean
Paleoproterozoic

detached and thrust over the Archean parautochthon creating a duplex (Figure 7.1 C). These events were followed by years of erosion exhuming most of the duplex, however, the limits of northwestward thrusting can be identified based on klippen that were not completely removed during exhumation.

The Lac Booth klippe, the Lac Watson nappe and the Mattawa klippe form the upper layer of a duplex thrust sheet and are the remnants of the northwestard thrusted APB. All of these allochthonous units are bounded by crustal units with a reworked Archean affinity indicating that the reworked Archean parautochthon was thrust to the northwest under the APB. The distribution of Nd-model ages also indicates that the reworked Archean parautochthon was thrust over the pristine Archean parautochthon. The Tomiko domain in the northern region of the study area exclusively hosts crustal units with Archean Nd-model ages whereas all of the rock units outside of this domain have a reworked Archean Nd-model age range. Hence, the Tomiko domain represents an area where the Grenville was so deeply exhumed, the pristine Archean parautochthon reached the surface. A Nd-model age boundary can be drawn between these distinct crustal units, however, contrarily to Ketchum and Davidson (2000), this boundary does not represent the ABT.

A similar scenario for the evolution of the Grenville Province is seen in western Labrador. Here the Molson Lake terrane was thrust over the Gagnon terrane (Rivers et al., 1993) in a similar manner to the overthrusting of the APB over the Paleoproterozoic parautochthon and the reworked Archean parautochthon in the present study area. Northwestward thrusting of the Molson Lake terrane resulted in basal décollment and northwestward thrusting in the underlying Gagnon terrane (Rivers et al., 1993). Although the Molson Lake terrane forms the southeast portion of the parautochthon in Labrador, this tectonic event is equivalent to the northwestward thrusting of the APB causing detachment and northwestward thrusting of the underlying reworked Archean parautochthon.

The last significant tectonic event to occur within the region was the development of the Mattawa fault, which is estimated to have occurred at approximately 0.6 Ga based on associated plutonic ages (Higgins, 1982) (Figure 7.1 D). The location of the Mattawa fault has been controlled by an ancient suture separating the reworked Archean parautochthon from the Paleoproterozoic parautochthon based on the distribution of Nd-model ages in the southern section of the field area.

7.2 Conclusions

The Grenville Province in the vicinity of Mattawa, Ontario represents a region with a complex geological history where tectonic boundaries have been obscured by intense metamorphism. However, through the indirect means of an isotopic system such as the Sm-Nd system, coupled with aeromagnetic data as an additional constraint, the evolution of the province in such geologically complex regions can be reconstructed. Differentiating between distinct metabasic rock types can be used to determine whether crustal units are allochthonous or autochthonous but cannot provide the location of first-order tectonic boundaries without another constraint. Therefore, when mapping tectonic boundaries in such geologically complex regions, multiple techniques provide the evidence necessary to correctly identify the locations of crustal boundaries.

BIBLIOGRAPHY

Arndt, N. T. and Goldstein, S. L. 1987. Use and abuse of crust-formation ages. Geology, **15**: 893-895.

Briggs, I. C. 1974. Machine contouring using minimum curvature. Geophysics, **39(1)**: 39-48.

Corrigan, D., Culshaw, N. G. and Mortensen, J. K. 1994. Pre-Grenvillian evolution and Grenville overprinting of the Parautochthonous Belt in Key Harbour, Ontario: U-Pb and field constraints. Canadian Journal of Earth Sciences, **31**: 583-596.

Culshaw, N. G., Jamieson, R., Ketchum, J., Reynolds, P. H. Wodicka, N., Heaman, L. and Krogh, T. 1991. History of the Central Gneiss Belt, Grenville Province, along Georgian Bay, Ontario. Lithoprobe Abitibi-Grenville Project, Workshop Report 3: 73-76.

Davidson, A. 1998a. An overview of Grenville Province geology, Canadian Shield; Chapter 3 in Geology of the Precambrian Superior and Grenville Provinces and Precambrian fossils in North America, (co-ord) S. B. Lucas and M. R. St-Onge; Geological survey of Canada, Geology of Canada, no. 7, p. 205-270 (also Geological Society of America, The geology of North America, v. C-1).

DePaolo, D. J. 1981. Neodymium isotopes in the Colorado Front Range and crust-mantle evolution in the Proterozoic. Nature, **291**: 193-196.

DePaolo, D. J. and Wasserburg, G. J. 1976. Nd isotopic variations and petrogenetic model. Geophys. Res. Lett., **3**: 249-252.

DeWolf, C. P., and Mezger, K. 1994. Lead isotope analyses of leached feldspars: constraints on the early crustal history of the Grenville Orogen. Geochimica Cosmochimica. Acta, **58**: 5537-5550.

Dickin, A. P. 1995. Comment on "Lead isotope analyses of leached feldspars: constraints on the early crustal history of the Grenville Orogeny" by C. P. DeWolf and K. Mezger. Geochimica et Cosmochimica Acta, **59**: 5233-5234.

Dickin, A. P. 1997. Radiogenic Isotope Geology. Cambridge University Press, 490 p.

Dickin, A. P. 1998a. Nd isotope mapping of a cryptic continental suture, Grenville Province of Ontario. Precambrian Research, **91**: 433-444.

Dickin, A. P. 2000. Crustal formation in the Grenville Province: Nd isotopic evidence. Canadian Journal of Earth Sciences, **37**: 165-181.

Dickin, A. P. and Guo, A. 2001. The location of the Allochthon Boundary Thrust and the Archean-Proterozoic suture in the Mattawa area of the Grenville Province: Nd isotope evidence. Precambrian Research, **107**: 31-43.

Dickin, A. P., and Higgins, M. 1992. Sm/Nd evidence for a major 1.5 Ga crust-forming event in the central Grenville province. Geology, **20**: 137-140.

Dickin, A. P., and McNutt, R. H. 1989. Nd model age mapping of the southeast margin of the Archean Foreland in the Grenville Province of Ontario. Geology, **17**: 299-302.

Easton, R. M. 1986. Geochronology of the Grenville Province in Moore, J. M., Davidson, A., Baer, A. J., eds., The Grenville: Geological Association of Canada Special Paper 31, p. 127-173.

Easton, R. M. 1988. Regional mapping and stratigraphic studies, Grenville Province, with some notes on mineralization; in Summary of Field Work and Other Activities 1988; Ontario Geological Survey, Miscellaneous Paper 141, p. 300-308.

Easton, R. M. 1992. The Grenville Province and the Proterozoic history of central and southern Ontario; in Geology of Ontario, (ed.) P. C. Thurston, H. R. Williams, R. H. Sutcliffe, and G. M. Scott; Ontario Geological Survey, Special Volume 4, pt. 2, p. 715-904.

Gariepy, C., Verner, D. and Doig, R. 1990. Dating Archean metamorphic minerals southeast of the Grenville Front, western Quebec, Using Pb isotopes. Geology, **18**: 1078-1081.

Guo, A. and Dickin, A. P. 1996. The southern limit of Archean crust and significance of rocks with Paleoproterozoic model ages: Nd model age mapping in the Grenville Province of western Quebec. Precambrian Research **77**: 231-241.

Higgins, M. D. 1982. Magmatism in the Grenville Province Since the Grenville Orogeny. Geoscience Canada **9**: 118-121.

Hoffman, P. F. 1989. Precambrian geology and tectonic history of North America. In: Geology of North America., Geological Society of America, Ch 16.

Holmden, C. and Dickin, A. P. 1995. Paleoproterozoic crustal history of the southwestern Grenville Province: evidence from Nd isotopic mapping. Canadian Journal of Earth Sciences, **32**: 472-485.

Indares, A., Dunning, G. 1997. Metamorphic constraints on the evolution of the gneisses from the parautochthonous and allochthonous polycyclic belts, Grenville Province, western Quebec. Canadian Journal of Earth Sciences, **34**: 357-370.

Kay, G. M. 1942. Ottawa-Bonnechere graben and the Lake Ontario homocline. Bulletin of the Seismological Society of America, **53**: p. 585.

Kellet, R. L., Barnes, A. E., Rive, M. 1994. The deep structure of the Grenville front: a new perspective from western Quebec. Canadian Journal of Earth Sciences, **31**: 282-292.

Ketchum, J. W. F. 1994. Extensional shear zones and lithotectonic domains in the southwest Grenville orogen: structure, metamorphism, and U-Pb geochronology of the Central Gneiss belt near Pointe-au-Baril, Ontario. PhD. Thesis, Dalhousie University, Halifax, Nova Scotia.

Ketchum, J. W. F. and Davidson, A. 2000. Crustal architecture and tectonic assembly of the Central Gneiss Belt, southwestern Grenville Province, Canada- a new interpretation. Canadian Journal of Earth Sciences, **37**: 217-234.

Korkisch, J. 1989. Handbook of ion exchange resins: their application to inorganic analytical chemistry, v. 1, CRC press, Inc, Florida, pp. 301.

Krogh, T. E. 1989. U-Pb systematics of zircon and titanite in metasediments and gneisses near the Grenville Front, Ontario. Geological Association of Canada, Programs with Abstracts, **14**: A52.

Krogh, T. E., Culshaw, N., and Ketchum, J. 1992. Multiple ages of metamorphism and deformation in the Parry Sound-Pointe au Baril area. Lithoprobe Abitibi-Grenville Workshop IV, Report 33, p. 39.

Logan, W. E. 1847. Report of progress for the year 1845-6; Geological Survey of Canada, p. 1-98.

Lumbers, S. B. 1976. Mattawa-Deep River area (western half), District of Nipissing, Ontario Division of mines, Preliminary Map P. 1196, Geological Series, scale 1: 63,360.

Lyall, H. B., 1959. Rapport Preliminaire sur la Region de McLachlin-Booth. Ministere des Mines, Quebec. Rpt. No. 391.

Martin, C. L. 1992. Mid-proterozoic evolution of the Grenville Belt: evidence from Neodymium isotopic mapping, Bancroft, Ontario. Unpublished B.Sc. Thesis, McMaster University, Hamilton, Ontario, 75p.

Minty, B. R. S. 1991. Simple micro-levelling for aeromagnetic data. Exploration Geophysics, **22**: 591-592.

Moorbath, S., Whitehouse, M. J., and Kamber, B. S. 1997. Extreme Nd-isotope heterogeneity in the early Archaean-fact or fiction? Case histories from northern Canada and West Greenland. Chemical Geology, **57**: 63-86.

Nelson, B. K. and DePaolo, D. J., 1985. Rapid production of continental crust 1.7-1.9 b.y. ago: Nd isotope evidence from the basement of the North American mid-continent. Geological Society of America Bulletin, **96**: 746-754.

North, R. B. 2001. Nd model age mapping of the central gneiss belt in the western Grenville province of Ontario, Canada. M.Sc. thesis, McMaster University, Hamilton, Ontario, p. 104.

Rive, M. 1973a. Geologie de la region des lacs Beauchene et Blue. Ministere des Richesses Naturelles, Quebec. Rpt. No. 580.

Rive, M. 1973b. Geologie de la region des lacs Ogascanane et Sairs. Ministere des Richesses Naturelles, Quebec. Rpt. No. 606.

Rivers, T., Martignole, J., Gower, C. F., and Davidson, A. 1989. New tectonic divisions of the Grenville Province, southeastern Canadian Shield. Tectonics, **8**: 63-84.

Rivers, T., van Gool, J. A. M., and Connelly, J. N. 1993. Contrasting tectonic styles in the northern Grenville Province: implications for the dynamics of orogenic fronts. Geology, **21**: p. 1127-1130.

Sabourin, R. –J. –E, 1960. Rapport Preliminaire sur la Region de pommeroy-Bellefeuille. Ctoral District. Ministere des Mines, Quebec. Rpt. no. 423.

Thirlwall, M. F. 1982. A triple filament method for rapid and precise analysis of rare-earth elements by isotope dilution. Chemical Geology, **35**: 155-166.

Van Breemen, O., Davidson, A., Loveridge, W. D., and Sullivan, R. W. 1986. U-Pb zircon geochronology of the Grenville tectonites, granulites and igneous precursors, Parry Sound, Ontario. In: The Grenville Province. Edited by J. M. Moore, A. Davidson, and A. J. Baer. Geological Association of Canada Special Paper 31, pp. 191-207.

Wynne-Edwards, H. R. 1976. Proterozoic ensialic orogenesis: the millipede model of ductile plate tectonics; American Journal of Science, **276**: 927-953.

APPENDIX A

ANALYTICAL PROCEDURES

A.1 Introduction

The analytical procedures for the geochronological analysis of Sm-Nd can be divided into four main subgroups. These being: 1) Rock sampling, 2) Rock crushing, 3) Dissolution and column chromatography, and 4) Mass spectrometry. These groups will be discussed in their order of operation.

A.2 Rock Sampling

Rock samples were collected from road outcrops, logging roads, rivers and small lakes within the entire field area. Samples of homogenous orthogneiss were collected weighing approximately between 5 and 10 kg. These rocks were located in terranes, which have undergone high-grade metamorphism, which enhances the difficulty of collecting a sample that is homogenous and representative of the country rock. As a result, caution was taken in the field to extract homogenous rock that was fresh and not considered to have undergone any intensive weathering.

A.3 Rock Crushing

The main objective of rock crushing is to remove remaining weathered portions from the rock sample, to achieve a small amount of uncontaminated sample that is representative of the rock in the field. Initially, in the rock crushing laboratory, rock samples are brushed heavily with a wire brush to remove any earth dust from the rock. The rocks are then split on a hydraulic jaw splitter into cubic pieces, no bigger than approximately 64 cm^3. While splitting, remaining weathered bits are removed and trashed. Likewise, any significant vein intrusion that is thought not to be a part of the original chemistry of the rock is also removed and thrown out. Following rock splitting, the rocks were then crushed into gravel sized particles in a jaw crusher. To avoid contamination at this stage, a small amount of sample was put through the jaw crusher and discarded. This pre-contaminated the jaw crusher to ensure that the collected gravel was not contaminated by any other samples, which have previously been through the jaw crusher. The collected gravel was then split several times on a table top splitter until only a small amount of gravel remained. This remaining gravel was placed in a tungsten carbide disc mill and placed on a shatterbox and pulverized into fine grained sand for approximately 3 or 4 minutes. This sand was dumped out of the disc mill onto a piece of paper and divided in half. Half of the sand was placed back in the disc mill and placed back on the shatter box for another 3 or 4 minutes and the other half was discarded. When the shatterbox was finished, the fine grained sand was placed in a glass jar and taken up to the clean chemistry lab to undergo dissolution.

The rock crushing lab generates a high amount of rock dust and extra precaution was taken to prevent following samples from being contaminated. While rocks were being put through the jaw crusher and being split, an air vacuum was functioning to remove the majority of the airborne particles. Between samples, the jaw crusher, rock splitter, sample divider, and disc mill set were vacuumed thoroughly and wiped with dustless tissue to remove any remaining particles that could be exposed to consecutive samples.

A.4 Dissolution and Column Chromatography

The objective of the dissolution stage is to dissolve all of the organic and silicate compounds from the sample and then separate Nd and Sm from the sample in the column chromatography stage. All dissolution and cation chromatography steps were carried out in a clean chemistry lab to prevent the samples from being contaminated from airborne dust particles. Prior to dissolution, 70 to 150 mg of sample was accurately weighed on a balance and placed in a teflon bomb, which had all of its static electricity removed. This sample was then dissolved in 10 ml of concentrated hydrofluoric acid (HF) and the bomb was safely sealed. The teflon bomb was then placed in a safety jacket and placed in an oven for 3 days at 140°C. After the 3 days, the bombs were carefully removed from the oven and allowed to cool. Once they were cool, all of the HF was evaporated off the sample on hot plates overnight. The sample was then dissolved in 10 ml of concentrated nitric acid (HNO_3) and once again evaporated. Finally, the remaining sample was redissolved in 5mL of 6M hydrochloric acid (HCl) and placed back in the safety jackets and returned to remain in the oven overnight.

The following day, the bombs were removed from the oven and allowed to cool. They were then opened and diluted with 10 ml of milli-Q water and resealed and shaken vigorously to homogenize the solution. The solutions were then split and spiked. For each sample, the weight of the bomb and solution was recorded. Half of the solution was poured off into a separate 15 ml teflon beaker and the weight of the bomb and the solution was recorded. Finally, the 15 ml beakers were spiked with a mixed REE spike that was enriched in Sm and Nd. Approximately 5 drops of the spike was added to the each beaker. Both the spiked (ID) and unspiked (IR) solutions were then evaporated on hot plates or under heat lamps and redissolved in 2 ml of 2.5 M HCl. These solutions were then transferred into test tubes and centrifuged for 10 minutes and put aside for column chromatography.

There are two stages in the process of column chromatography. In the first stage, the solution is eluted through cation exchange columns and all of the Rare Earth Elements (REEs) are collected. Secondly, the solution of REEs is eluted through a reverse phase anion column, where Sm and Nd are collected separately. These two stages will be discussed separately.

Cation Exchange Chromatography: These columns contained approximately 14 cm of Dowex Bio-Rad AG 50W (200 - 400 mesh) resin. A full description of ion exchange resins can be found in Korkisch (1989). 1 ml of the 2.5 M HCl sample was loaded onto these columns and then eluted further in with 2 ml of 2.5 M HCl. The major elements, such as Na, Ca, and K, were removed by eluting the sample with 34 ml of 2.5 M HCl and 20 ml of 2 M HNO_3. Finally, the REEs were collected with 12 ml of 7.5 M HNO_3. This solution was then evaporated to dryness under the heat lamps and the sample was redissolved in 1 ml of 0.3 M HCl and put aside for the reverse phase anion column.

REE Chromatography: These columns are often referred to as "reverse phase" columns due to the fact that the light REEs are removed first, before the heavy REEs. These quartz columns contain a hexyl di-ethyl hydrogen phosphate resin, which is coated onto teflon beads. 1 ml of the 0.3 M HCl sample solution was loaded onto these columns and washed in with 2 ml of 0.3 M HCl. The sample was then eluted with 24 ml of 0.3 M HCl and Nd was removed with 12 ml of 0.3 M HCl. Sm from the spiked solution was further eluted with 4 ml of 1 M HCl and collected with 12 ml of 1 M HCl. This procedure produces three solutions: a solution to measure the Nd isotopic ratio ($^{143}Nd/^{144}Nd$), a solution with the heavy REE for isotope dilution analysis of Sm, and a solution of the light REE for isotope dilution of Nd. These solutions were evaporated to dryness under the heat lamps. Finally, the remaining sample was dissolved in one drop of 0.0003 M H_3PO_4 and partially evaporated. This step removes the entire remaining residue from the sample and also acts as an adhesive for when the samples are to be loaded onto the beads for mass spectrometry.

A.5 Mass Spectrometry

The samples from the clean lab were loaded onto outgassed glass beads, which had a Tantalum side filament and a Rhenium centre filament. The sample was dissolved in approximately 1/2 a microlitre of 0.3 M H_3PO_4 and loaded onto the Tantalum side filament. Thirwall (1982) gives a complete description of the use of triple filament beads in isotope dilution analysis of the REEs. This solution was then dried by exposing the filament to an electrical current between 2.0-2.5 amps.

All isotope ratios were measured using a VG isomass 354 solid source mass spectrometer at a source pressure no greater than 2.7×10^{-7} bars. The whole rock content of Sm and Nd (isotope dilution) was measured using a ^{149}Sm-^{150}Nd mixed spike. The La Jolla standard from previous studies produced a mean of 0.511854 ± 0.00002 (2σ) (Dickin and McNutt, 1989, Guo and Dickin, 1995, Martin, 1992, etc.). All isotope dilution analyses with within run precision > 0.02 % were rejected and all Nd isotope ratio analyses with within run precision > 0.01/mil were rejected. Based on replicated analyses, these errors were found to represent a Nd-model age error of 20 Myr (Dickin and McNutt, 1989, Holmden and Dickin, 1995, Guo and Dickin, 1995, Martin, 1992).

Table A.1: La Jolla Standard Analyses ($^{143}Nd/^{144}Nd$, May 2000 to December 2001)

	$^{143}Nd/^{144}Nd$	Standard Error (/mil)		$^{143}Nd/^{144}Nd$	Standard Error (/mil)
1	0.511841	0.009	13	0.511872	0.038
2	0511863	0.011	14	0.511864	0.012
3	0511841	0.016	15	0.511866	0.010
4	0.511873	0.013	16	0.511875	0.013
5	0.511845	0.011	17	0.511864	0.010
6	0.511866	0.011	18	0.511858	0.010
7	0.511891	0.010	19	0.511852	0.012
8	0.511863	0.009	20	0.511856	0.011
9	0.511863	0.011	21	0.511868	0.009
10	0.511859	0.011	22	0.511868	0.012
11	0.511854	0.007	23	0.511875	0.011
12	0.511857	0.011			

Average value of all 23 $^{143}Nd/^{144}Nd$ ratios: 0.511862 ± 0.000012 (2σ, population)